Optimized Sensor Collaboration for Estimation of Temporally Correlated Parameters

Sijia Liu *Member, IEEE,* Swarnendu Kar, *Member, IEEE,* Makan Fardad, *Member, IEEE,* and Pramod K. Varshney *Fellow, IEEE*

***Abstract*—In this paper, we aim to design the optimal sensor collaboration strategy for the estimation of time-varying parameters, where collaboration refers to the act of sharing measurements with neighboring sensors prior to transmission to a fusion center. We begin by addressing the sensor collaboration problem for the estimation of uncorrelated parameters. We show that the resulting collaboration problem can be transformed into a special nonconvex optimization problem, where a difference of convex functions carries all the nonconvexity. This specific problem structure enables the use of a convex-concave procedure to obtain a near-optimal solution. When the parameters of interest are temporally correlated, a penalized version of the convex-concave procedure becomes well suited for designing the optimal collaboration scheme. In order to improve computational efficiency, we further propose a fast algorithm that scales gracefully with problem size via the alternating direction method of multipliers. Numerical results are provided to demonstrate the effectiveness of our approach and the impact of parameter correlation and temporal dynamics of sensor networks on estimation performance.**

***Index Terms*—Distributed estimation, sensor collaboration, convex-concave procedure, semidefinite programming, ADMM, wireless sensor networks.**

I. Introduction

Wireless sensor networks (WSNs) consist of a large number of spatially distributed sensors that often cooperate to perform parameter estimation; example applications include environment monitoring, source localization and target tracking [1]–[3]. Under limited resources, such as limited communication bandwidth and sensor battery power, it is important to design an energy-efficient architecture for distributed estimation. In this paper, we employ a WSN to estimate time-varying parameters in the presence of inter-sensor communication that is referred to as sensor collaboration. Here sensors are allowed to update their measurements by taking a linear combination of the measurements of those they interact with prior to transmission to a fusion center (FC). The presence of sensor collaboration smooths out the observation noise, thereby improving the quality of the signal and the eventual estimation performance.

Early research efforts [4]–[13] focused on the problem of distributed inference (estimation or detection) in the absence of sensor collaboration, where an amplify-and-forward transmission strategy is commonly used. In [4], the problem of designing optimal power amplifying factors (also known as power allocation problem) was studied for distributed estimation over an orthogonal multiple access channel (MAC). In [5], the power allocation problem was addressed when the MAC is coherent, where sensors coherently form a beam into a common channel received at the FC. In [6], a likelihood-based multiple access communication strategy was proposed for estimation, and was proved to be asymptotically efficient as the number of sensors increases. In [7], feedback signals were studied to combat uncertainty in the observation model for distributed estimation with coherent MAC. In [8], distributed detection problem was studied in the setting of identical Gaussian multiple access channels (without fading). It was shown that the centralized error exponent can be achieved via the transmission of the log-likelihood ratio as the number of sensors approaches infinity. Further in [9]–[11], asymptotic detection performance was studied over multiaccess fading channels. In [12], the problem of power allocation was studied for distributed detection using a MAC. In [13], the impact of nonlinear bounded transmission schemes was studied on distributed detection and estimation. In the aforementioned literature [4]–[13], the act of inter-sensor communication was not considered. In contrast, here we seek the optimal sensor collaboration scheme for the estimation of temporally correlated parameters.

Recently, the problem of distributed estimation with sensor collaboration has attracted attention [14]–[22]. In [14], the optimal power allocation strategy was found for a fully connected network, where all the sensors are allowed to collaborate, namely, share their measurements with the other sensors. It was shown that sensor collaboration results in significant improvement of estimation performance compared with the conventional amplify-and-forward transmission scheme. In [15] and [16], optimal power allocation schemes were found for star, branch and linear network topologies. In [17], the sensor collaboration problem was studied for parameter estimation via the best linear unbiased estimator. In [18]–[20], the problem of sensor collaboration was studied given an arbitrary collaboration topology. It was observed that even

S. Liu was with Syracuse University. Now he is with the Department of Electrical Engineering and Computer Science, University of Michigan, Ann Arbor, MI 48109, USA. Email: lsjxjtu@umich.edu.

S. Kar is with New Devices Group, Intel Corporation, Hillsboro, Oregon, 97124 USA. Email: swarnendu.kar@intel.com.

M. Fardad and P. K. Varshney are with the Department of Electrical Engineering and Computer Science, Syracuse University, Syracuse, NY, 13244 USA. Email: {makan, varshney}@syr.edu.

The work of S. Liu and P. K. Varshney was supported by the U.S. Air Force Office of Scientific Research under grants FA9550-10-1-0458. The work of M. Fardad was supported by the National Science Foundation under awards EAGER ECCS-1545270 and CNS-1329885.

a partially connected network can yield performance close to that of a fully connected network. In [21] and [22], nonzero collaboration costs were taken into account, and a sparsity inducing optimization framework was proposed to jointly design both sensor selection and sensor collaboration schemes.

In the existing literature [14]–[22], sensor collaboration was studied in static networks, where sensors take a single snapshot of the static parameter, and then initiate sensor collaboration protocols designed in the setting of single-snapshot estimation. In contrast, here we study the problem of sensor collaboration for the estimation of *temporally-correlated* parameters in *dynamic* networks that involve, for example, time-varying observation and channel gains. Solving such a problem is also motivated by real-life applications, in which the physical phenomenon to be monitored such as daily temperature, precipitation, soil moisture and seismic activities [23]–[25] is temporally correlated. For example, when monitoring daily temperature variations, temperatures at different times of the day are strongly correlated, e.g., a cold morning is likely to be followed by a cold afternoon.

Due to the presence of temporal dynamics and parameter correlation, optimal sensor collaboration schemes at multiple time steps are coupled with each other, and thus pose many challenges in problem formulation and optimization compared to the existing work [14]–[22]. For example, when parameters of interest are temporally correlated, expressing the estimation distortion in a succinct closed form (with respect to the collaboration variables) is not straightforward. It should be pointed out that even for uncorrelated parameters, finding the optimal collaboration scheme for each time step is nontrivial since energy constraints are temporally inseparable. In this paper, we seek the optimal sensor collaboration scheme by minimizing the estimation distortion subject to individual energy constraints of sensors in the presence of (a) temporal dynamics in system, (b) temporal correlation of parameter, and (c) energy constraints in time.

Besides [14]–[22], our work is also related to but quite different from the problem of consensus-based decentralized estimation [26]–[32]. The common idea in [26]–[32] is that the task of centralized estimation can be performed using local estimators at sensors together with inter-sensor communications. It was shown in [31] and [32] that the success of decentralized estimation is based on the fact that the global estimation cost with respect to the parameter of interest can be converted into a sum of local cost functions subject to consensus constraints. Different from [26]–[32], the focus of this paper is to design the optimal energy allocation strategy (namely, the collaboration weights), rather to find the optimal estimate. Here tasks of estimation and optimization are completed at an FC. Moreover, the studied sensor network is not necessarily connected. An extreme case is that in the absence of inter-sensor communication, the proposed sensor collaboration problem would reduce to the conventional power allocation problem (based on the amplify-and-forward transmission strategy) [4], [5]. Therefore, our problem is different from the consensus-based decentralized estimation problem, in which the network is assumed to be connected so that the consensus of estimate at local sensors can be achieved.

In our work, design of the optimal collaboration scheme is studied under two scenarios: a) parameters are temporally uncorrelated or prior knowledge about temporal correlation is not available, and b) parameters are temporally correlated. When parameters are uncorrelated, we derive the closed form of the estimation distortion with respect to sensor collaboration variables, which is in the form of a sum of quadratic ratios. We show that the resulting sensor collaboration problem is equivalent to a nonconvex quadratically constrained problem, in which the difference of convex functions carries all the nonconvexity. This specific problem structure enables the use of convex-concave procedure (CCP) [33] to solve the sensor collaboration problem in a numerically efficient manner.

When parameters of interest are temporally correlated, expressing the estimation error as an explicit function of the collaboration variables becomes difficult. In this case, we show that the sensor collaboration problem can be converted into a semidefinite program together with a (nonconvex) rank-one constraint. After convexification, the method of penalty CCP [34] becomes well-suited for seeking the optimal sensor collaboration scheme. However, the proposed algorithm is computationally intensive for large-scale problems. To improve computational efficiency, we develop a fast algorithm that scales gracefully with problem size by using the alternating direction method of multipliers (ADMM) [35].

We summarize our contributions as follows.

- We propose a tractable optimization framework for the design of the optimal collaboration scheme that accounts for parameter correlation and temporal dynamics of sensor networks.
- We show that the problem of sensor collaboration for the estimation of temporally uncorrelated parameters can be solved as a special nonconvex problem, where the only source of nonconvexity can be isolated to a constraint that contains the difference of convex functions.
- We provide valuable insights into the problem structure of sensor collaboration with correlated parameters, and propose an ADMM-based algorithm for improving the computational efficiency.

The rest of the paper is organized as follows. In Section II, we introduce the collaborative estimation system, and present the general formulation of the optimal sensor collaboration problem. In Section III, we discuss two types of sensor collaboration problems for the estimation of temporally uncorrelated and correlated parameters. In Section IV, we study the sensor collaboration problem with uncorrelated parameters. In Section V, we propose efficient optimization methods to solve the sensor collaboration problem with correlated parameters. In Section VI, we demonstrate the effectiveness of our approach through numerical examples. Finally, in Section VII we summarize our work and discuss future research directions.

II. System Model

In this section, we introduce the collaborative estimation system and formulate the sensor collaboration problem considered in this work. The task here is to estimate a time-varying parameter θ_k over a time horizon of length K. In the estimation system, sensors first accquire their raw measurements

via a linear sensing model, and then update their observations through spatial collaboration, where collaboration refers to the act of sharing measurements with neighboring sensors. The collaborative signals are then transmitted through a coherent MAC to the FC, which finally determines a global estimate of θ_k for $k \in [K]$. The overall architecture of the collaborative estimation system is shown in Fig. 1.

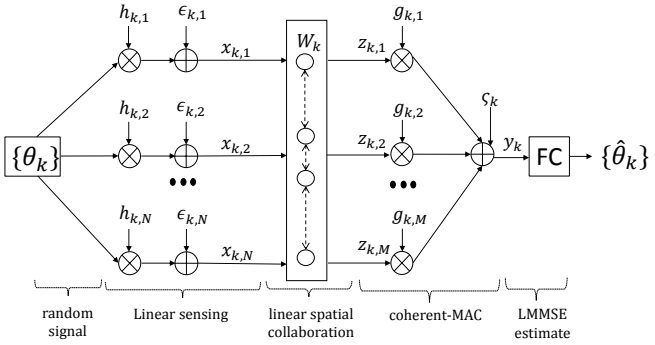

Fig. 1: Collaborative estimation architecture.

The vector of measurements from N sensors at time k is given by the linear sensing model

$$\mathbf{x}_k = \mathbf{h}_k \theta_k + \boldsymbol{\epsilon}_k,\ k \in [K], \tag{1}$$

where for notational simplicity, let $[K]$ denote the integer set $\{1, 2, \ldots, K\}$, $\mathbf{x}_k = [x_{k,1}, \ldots, x_{k,N}]^T$ is the vector of measurements, $\mathbf{h}_k = [h_{k,1}, \ldots, h_{k,N}]^T$ is the vector of observation gains, without loss of generality θ_k is assumed to be a random process with zero mean and variance σ_θ^2, $\boldsymbol{\epsilon}_k = [\epsilon_{k,1}, \ldots, \epsilon_{k,N}]^T$ is the vector of Gaussian noises with i.i.d variables $\epsilon_{k,n} \sim \mathcal{N}(0, \sigma_\epsilon^2)$ for $k \in [K]$ and $n \in [N]$.

After linear sensing, each sensor may pass its observation to other sensors for collaboration prior to transmission to the FC. With a relabelling of sensors, we assume that the first M sensors (out of a total of N sensor nodes) communicate with the FC. Collaboration among sensors is represented by a known matrix $\mathbf{A} \in \mathbb{R}^{M \times N}$ with zero-one entries, namely, $A_{mn} \in \{0, 1\}$ for $m \in [M]$ and $n \in [N]$. Here we call $\mathbf{A}$ a topology matrix, where $A_{mn} = 1$ signifies that the nth sensor shares its observation with the mth sensor, and $A_{mn} = 0$ indicates the absence of a collaboration link from the nth sensor to the mth sensor. Note that $\mathbf{A}$ is essentially a truncated adjacency matrix. The bidirectional communication link between two sensors indicates that the underlying graph of the network is directed but not necessarily connected. In particular, the network given by $A_{mn} = 0$ for $n \neq m$ corresponds to the amplify-and-forward transmission strategy considered in [4].

Based on the topology matrix, the sensor collaboration process at time k is given by

$$\begin{aligned} &\mathbf{z}_k = \mathbf{W}_k \mathbf{x}_k,\ k \in [K] \\ &\mathbf{W}_k \circ (\mathbf{1}_M \mathbf{1}_N^T - \mathbf{A}) = \mathbf{0}, \end{aligned} \tag{2}$$

where $\mathbf{z}_k = [z_{k,1}, z_{k,2}, \ldots, z_{k,M}]^T$, $z_{k,m}$ is the signal after collaboration at sensor m and time k, $\mathbf{W}_k \in \mathbb{R}^{M \times N}$ is the collaboration matrix that contains collaboration weights (based on the energy allocated) used to combine sensor measurements at time k, $\circ$ denotes the elementwise product, $\mathbf{1}_N$ is the $N \times 1$ vector of all ones, and $\mathbf{0}$ is the $M \times N$ matrix of all zeros. In what follows, while refering to vectors of all ones and all zeros, their dimensions will be omitted for simplicity but can be inferred from the context. In (2), we assume that sharing of an observation is realized through an ideal (noiseless and cost-free) communication link. The proposed ideal collaboration model enables us to obtain explicit expressions for transmission cost and estimation distortion.

After sensor collaboration, the message $\mathbf{z}_k$ is transmitted through a coherent MAC so that the received signal y_k at the FC is a coherent sum [5]

$$y_k = \mathbf{g}_k^T \mathbf{z}_k + \varsigma_k,\ k \in [K], \tag{3}$$

where $\mathbf{g}_k = [g_{k,1}, g_{k,2}, \ldots, g_{k,M}]^T$ is the vector of channel gains, and ς_k is temporally independent Gaussian noise with zero mean and variance σ_ς^2.

From (1) – (3), the vector of received signals at the FC can be compactly expressed as a linear function of parameters $\boldsymbol{\theta} = [\theta_1, \theta_2, \ldots, \theta_K]^T$,

$$\mathbf{y} = \mathbf{D}_W \mathbf{D}_h \boldsymbol{\theta} + \boldsymbol{\nu},\ \mathbf{D}_W := \mathrm{blkdiag}\{\mathbf{g}_k^T \mathbf{W}_k\}_{k=1}^K, \tag{4}$$

where $\mathbf{y} = [y_1, y_2, \ldots, y_K]^T$, $\boldsymbol{\nu} = [\nu_1, \nu_2, \ldots, \nu_K]^T$, $\nu_k := \mathbf{g}_k^T \mathbf{W}_k \boldsymbol{\epsilon}_k + \varsigma_k$, $\mathbf{D}_h := \mathrm{blkdiag}\{\mathbf{h}_k\}_{k=1}^K$, and $\mathrm{blkdiag}\{\mathbf{X}_i\}_{i=1}^n$ denotes the block-diagonal matrix with diagonal blocks $\mathbf{X}_1, \mathbf{X}_2, \ldots, \mathbf{X}_n$.

At the FC, we employ a linear minimum mean squared-error estimator (LMMSE) [36] to estimate $\boldsymbol{\theta}$, where we assume that the FC knows the observation gains, channel gains, and the second-order statistics of the parameters of interest and additive noises. The corresponding estimation error covariance is given by [36, Theorem 10.3]

$$\mathbf{P}_W = (\boldsymbol{\Sigma}_\theta^{-1} + \mathbf{D}_h^T \mathbf{D}_W^T \mathbf{D}_\nu^{-1} \mathbf{D}_W \mathbf{D}_h)^{-1}, \tag{5}$$

where $\boldsymbol{\Sigma}_\theta$ represents prior knowledge about the parameter correlation, particularly $\boldsymbol{\Sigma}_\theta = \sigma_\theta^2 \mathbf{I}_K$ for temporally uncorrelated parameters, $\mathbf{I}_K$ is the $K \times K$ identity matrix, and $\mathbf{D}_\nu := \sigma_\epsilon^2 \mathbf{D}_W \mathbf{D}_W^T + \sigma_\varsigma^2 \mathbf{I}_K$. It is clear from (5) that the estimation error covariance matrix is a function of collaboration matrices $\{\mathbf{W}_k\}$, and their dependence on $\{\mathbf{W}_k\}$ is through $\mathbf{D}_W$. This dependency does not lend itself to easy optimization of scalar-valued functions of $\mathbf{P}_W$ for design of the optimal sensor collaboration scheme. More insights into the LMMSE will be provided in Sec. III.

We next define the transmission cost of the mth sensor at time k, which refers to the energy consumption of transmitting the collaborative message $\mathbf{z}_k$ to the FC. That is,

$$\begin{aligned} T_m(\mathbf{W}_k) &= \mathbb{E}_{\theta_k, \boldsymbol{\epsilon}_k}[z_{k,m}^2] \\ &= \mathbf{e}_m^T \mathbf{W}_k (\sigma_\theta^2 \mathbf{h}_k \mathbf{h}_k^T + \sigma_\epsilon^2 \mathbf{I}_N) \mathbf{W}_k^T \mathbf{e}_m, \end{aligned} \tag{6}$$

for $m \in [M]$ and $k \in [K]$, where $\mathbf{e}_m \in \mathbb{R}^M$ is a basis vector with 1 at the mth coordinate and 0s elsewhere. In what follows, while refering to basis vectors and identity matrices, their dimensions will be omitted for simplicity but can be inferred from the context.

We now state the main optimization problem considered in this work for sensor collaboration

$$\begin{aligned} &\text{minimize} && \operatorname{tr}(\mathbf{P}_W) \\ &\text{subject to} && \sum_{k=1}^{K} T_m(\mathbf{W}_k) \le E_m, \qquad m \in [M] \\ &&& \mathbf{W}_k \circ (\mathbf{1}_M \mathbf{1}_N^T - \mathbf{A}) = \mathbf{0}, \quad k \in [K], \end{aligned} \tag{7}$$

where $\mathbf{W}_k$ is the optimization variable for $k \in [K]$, $\operatorname{tr}(\mathbf{P}_W)$ denotes the estimation distortion of using the LMMSE, $T_m(\mathbf{W}_k)$ is the transmission cost given by (6), E_m is a prescribed energy budget of the mth sensor, and $\mathbf{A}$ characterizes the network topology. The problem structure and the solution of (7) will be elaborated on in the rest of the paper.

We end this section with the following remarks.

Remark 1: In the system model, the assumption of known observation and channel gains can be further relaxed to that of given knowledge about their second-order statistics. Our earlier work [22] has shown that under this weaker assumption, we can obtain similar expressions of the linear estimator. In this paper, we assume the observation and channel models are known for ease of presentation and analysis.

Remark 2: Although sensor collaboration is performed with respect to a time-invariant (fixed) topology matrix $\mathbf{A}$, energy allocation in terms of the magnitude of nonzero entries in $\mathbf{W}_k$ is time varying in the presence of temporal dynamics of the sensor network. As will be evident later, the proposed sensor collaboration approach is also applicable to the problem with time-varying topologies.

III. Reformulation and Simplification Using Matrix Vectorization

In this section, we simplify problem (7) by exploiting the sparsity structure of the topology matrix and concatenating the nonzero entries of a collaboration matrix into a collaboration vector. There exist two benefits to using matrix vectorization: a) the topology constraint in (7) can be eliminated without loss of performance, which renders a less complex problem; b) the structure of nonconvexities is more easily revealed via such a reformulation.

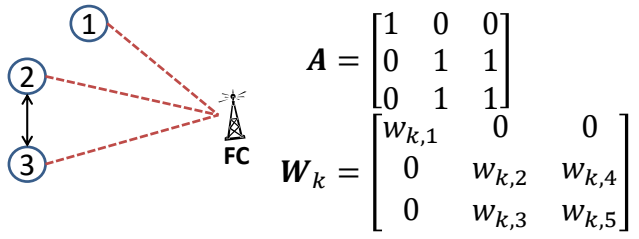

Fig. 2: Example of vectorization of $\mathbf{W}_k$.

In problem (7), the only optimization variables are the nonzero entries of collaboration matrices. We concatenate these nonzero entries (columnwise) into a collaboration vector

$$\mathbf{w}_k = [w_{k,1}, w_{k,2}, \ldots, w_{k,L}]^T, \tag{8}$$

where $w_{k,l}$ denotes the lth entry of $\mathbf{w}_k$, and L is the number of nonzero entries of the topology matrix $\mathbf{A}$. We note that given $w_{k,l}$, there exists a row index m_l and a column index n_l such that $w_{k,l} = [\mathbf{W}_k]_{m_l n_l}$, where $[\mathbf{X}]_{mn}$ (or X_{mn}) denotes the (m,n)th entry of a matrix $\mathbf{X}$. We demonstrate the vectorization of $\mathbf{W}_k$ through an example in Fig. 2, where we consider $N = 3$ sensor nodes, $M = 3$ communicating nodes, and 2 collaboration links.

A. Collaboration problem for the estimation of uncorrelated parameters

When the parameters of interest are uncorrelated, the estimation error covariance matrix (5) simplifies to

$$\begin{aligned} \mathbf{P}_W &= \left(\sigma_\theta^{-2}\mathbf{I} + \mathbf{D}_h^T \mathbf{D}_W^T (\sigma_\epsilon^2 \mathbf{D}_W \mathbf{D}_W^T + \sigma_\varsigma^2 \mathbf{I})^{-1} \mathbf{D}_W \mathbf{D}_h\right)^{-1} \\ &= \left(\sigma_\theta^{-2}\mathbf{I} + \operatorname{diag}\left\{ \frac{\mathbf{g}_k^T \mathbf{W}_k \mathbf{h}_k \mathbf{h}_k^T \mathbf{W}_k^T \mathbf{g}_k}{\sigma_\epsilon^2 \mathbf{g}_k^T \mathbf{W}_k \mathbf{W}_k^T \mathbf{g}_k + \sigma_\varsigma^2} \right\}_{k=1}^{K} \right)^{-1} \\ &= \operatorname{diag}\left\{ \frac{\sigma_\theta^2 \sigma_\epsilon^2 \mathbf{g}_k^T \mathbf{W}_k \mathbf{W}_k^T \mathbf{g}_k + \sigma_\theta^2 \sigma_\varsigma^2}{\sigma_\theta^2 \mathbf{g}_k^T \mathbf{W}_k \mathbf{h}_k \mathbf{h}_k^T \mathbf{W}_k^T \mathbf{g}_k + \sigma_\epsilon^2 \mathbf{g}_k^T \mathbf{W}_k \mathbf{W}_k^T \mathbf{g}_k + \sigma_\varsigma^2} \right\}_{k=1}^{K}, \end{aligned} \tag{9}$$

where $\operatorname{diag}\{a_k\}_{k=1}^K$ denotes a diagonal matrix with diagonal entries $a_1, a_2, \ldots, a_K$.

Let $\mathbf{w} \in \mathbb{R}^L$ be the vector obtained by stacking the nonzero entries of $\mathbf{W} \in \mathbb{R}^{M \times N}$ columnwise. Then

$$\mathbf{b}^T \mathbf{W} = \mathbf{w}^T \mathbf{B}, \tag{10}$$

where $\mathbf{b} \in \mathbb{R}^N$ is a coefficient vector, $\mathbf{B}$ is an $L \times N$ matrix whose (l,n)th entry is given by

$$B_{ln} = \begin{cases} b_{m_l} & n = n_l \\ 0 & \text{otherwise}, \end{cases} \tag{11}$$

and the indices m_l and n_l are such that $w_l = W_{m_l n_l}$ for $l \in [L]$. The proof of equation (10) is given in Appendix A for the sake of completeness.

From (9) and (10), the objective function of problem (7) can be rewritten as

$$\phi(\mathbf{w}) := \operatorname{tr}(\mathbf{P}_W) = \sum_{k=1}^{K} \frac{\sigma_\theta^2 \sigma_\epsilon^2 \mathbf{w}_k^T \mathbf{R}_k \mathbf{w}_k + \sigma_\theta^2 \sigma_\varsigma^2}{\mathbf{w}_k^T \mathbf{S}_k \mathbf{w}_k + \sigma_\varsigma^2}, \tag{12}$$

where we used the fact that $\mathbf{g}_k^T \mathbf{W}_k = \mathbf{w}_k^T \mathbf{G}_k$, i.e., $\mathbf{G}_k$ is derived from $\mathbf{g}_k$ in the same way that $\mathbf{B}$ is derived from $\mathbf{b}$ in (10), and $\mathbf{S}_k := \mathbf{G}_k(\sigma_\theta^2 \mathbf{h}_k \mathbf{h}_k^T + \sigma_\epsilon^2 \mathbf{I}) \mathbf{G}_k^T$.

Moreover, the transmission cost (6) can be rewritten as

$$\begin{aligned} T_m(\mathbf{w}_k) &:= \mathbf{w}_k^T \mathbf{Q}_{k,m} \mathbf{w}_k, \\ \mathbf{Q}_{k,m} &:= \mathbf{E}_m(\sigma_{\theta,k}^2 \mathbf{h}_k \mathbf{h}_k^T + \sigma_\epsilon^2 \mathbf{I}) \mathbf{E}_m^T, \end{aligned} \tag{13}$$

where $\mathbf{E}_m$ is defined as in (10) such that $\mathbf{e}_m^T \mathbf{W}_k = \mathbf{w}_k^T \mathbf{E}_m$. We remark that $\mathbf{Q}_{k,m}$ is positive semidefinite for $k \in [K]$ and $m \in [M]$.

From (12) and (13), the sensor collaboration problem for the estimation of temporally uncorrelated parameters becomes

$$\begin{aligned} &\text{minimize} && \phi(\mathbf{w}) \\ &\text{subject to} && \mathbf{w}^T \mathbf{Q}_m \mathbf{w} \le E_m, \ m \in [M], \end{aligned} \tag{P1}$$

where $\mathbf{w} = [\mathbf{w}_1^T, \mathbf{w}_2^T, \ldots, \mathbf{w}_K^T]^T$ is the optimization variable, $\phi(\mathbf{w})$ is the estimation distortion given by (12), and

$\mathbf{Q}_m := \text{blkdiag}\{\mathbf{Q}_{k,m}\}_{k=1}^K$. Note that (P1) cannot be decomposed in time since sensor energy constraints are temporally inseparable.

Compared to problem (7), the topology constraint in terms of $\mathbf{A}$ is eliminated without loss of performance in (P1) since the sparsity structure of the topology matrix has been taken into account while constructing the collaboration vector. In the special case of single-snapshot estimation (namely, $K = 1$), the objective function of (P1) simplifies to a single quadratic ratio. It has been shown in [18] and [22] that such a nonconvex problem can be readily solved via convex programming. In contrast, (P1) is a more complex nonconvex optimization problem, where the nonconvexity stems from the *sum* of quadratic ratios in the objective function. As indicated in [37] and [38], the Karush-Kuhn-Tucker (KKT) conditions of such a complex fractional optimization problem are intractable to solve to obtain the globally optimal solution (or all locally optimal solutions). Therefore, an efficient local optimization method will be proposed to solve (P1) in Sec. IV. Also, the efficacy of the proposed solution will be shown in Sec. VI via extensive numerical experiments.

B. Collaboration problem for the estimation of correlated parameters

When parameters are temporally correlated, the covariance matrix $\mathbf{\Sigma}_\theta$ is no longer diagonal and it is not straight forward to express the estimation error in a succinct form, as was done in (12). We recall from (5) that the dependence of the estimation error covariance on collaboration matrices is through $\mathbf{D}_W$. According to the matrix inversion lemma [36, A 1.1.3],

$$\begin{aligned}\mathbf{D}_W^T(\sigma_\epsilon^2\mathbf{D}_W\mathbf{D}_W^T + \sigma_\varsigma^2\mathbf{I})^{-1}\mathbf{D}_w \\ = \sigma_\epsilon^{-2}\mathbf{I} - (\sigma_\epsilon^2\mathbf{I} + \sigma_\epsilon^4\sigma_\varsigma^{-2}\mathbf{D}_W^T\mathbf{D}_W)^{-1}.\end{aligned} \tag{14}$$

Substituting (14) into (5), we obtain

$$\mathbf{P}_W = \left(\mathbf{C} - \sigma_\epsilon^{-2}\mathbf{D}_h^T(\mathbf{I} + \sigma_\epsilon^2\sigma_\varsigma^{-2}\mathbf{D}_W^T\mathbf{D}_W)^{-1}\mathbf{D}_h\right)^{-1} \tag{15}$$

with $\mathbf{C} := \mathbf{\Sigma}_\theta^{-1} + \sigma_\epsilon^{-2}\mathbf{D}_h^T\mathbf{D}_h$. According to the definition of $\mathbf{D}_W$ in (4), we obtain

$$\begin{aligned}\mathbf{D}_W^T\mathbf{D}_W &= \text{blkdiag}\{\mathbf{W}_k^T\mathbf{g}_k\mathbf{g}_k^T\mathbf{W}_k\}_{k=1}^K \\ &= \text{blkdiag}\{\mathbf{G}_k^T\mathbf{w}_k\mathbf{w}_k^T\mathbf{G}_k\}_{k=1}^K,\end{aligned} \tag{16}$$

where $\mathbf{G}_k$ has been introduced in the paragraph that proceeds (12).

Combining (15) and (16), we can rewrite the estimation error covariance as a function of the collaboration vector

$$\begin{aligned}\mathbf{P}_w := \Big(\mathbf{C} - \sigma_\epsilon^{-2}\,\text{diag}\left\{\mathbf{h}_k^T\left(\mathbf{I} + \sigma_\epsilon^2\sigma_\varsigma^{-2}\mathbf{G}_k^T\mathbf{w}_k\mathbf{w}_k^T\mathbf{G}_k\right)^{-1}\right. \\ \left.\cdot\,\mathbf{h}_k\right\}_{k=1}^K\Big)^{-1}.\end{aligned} \tag{17}$$

From (17), the sensor collaboration problem for the estimation of temporally correlated parameters becomes

$$\begin{aligned}&\text{minimize} && \text{tr}(\mathbf{P}_w) \\ &\text{subject to} && \mathbf{w}^T\mathbf{Q}_m\mathbf{w} \le E_m,\ m \in [M],\end{aligned} \tag{P2}$$

where $\mathbf{w} = [\mathbf{w}_1^T, \mathbf{w}_2^T, \ldots, \mathbf{w}_K^T]^T$ is the optimization variable.

We note that (P2) is a nonconvex optimization problem. We will show in Sec. V that the rank-one matrix $\mathbf{w}_k\mathbf{w}_k^T$ that appears in (17) is the source of nonconvexity. Compared to (P1), (P2) is more involved due to the presence of the parameter correlation. We will also show that (P2) can be cast as a particular nonconvex optimization problem, where the objective function is linear, and the constraint set is formed by convex quadratic constraints, linear matrix inequalities and nonconvex rank constraints. The presence of generalized inequalities (with respect to positive semidefnite cones) and rank constraints make KKT conditions complex and intractable to find the globally optimal solution. Instead, we will employ an efficient convexification method to find a locally optimal solution of (P2). The efficacy of the proposed optimization method will be empirically shown in Sec. VI.

We finally remark that both (P1) and (P2) are feasible optimization problems, namely, in the sense that an optimal solution exists for each of them. This can be examined as follows. First, there exists a non-empty constraint set. For example, $\mathbf{w}_k = \mathbf{0}$ is a feasible solution to (P1) and (P2). When $\mathbf{w}_k = \mathbf{0}$, the estimate of the unknown parameter is only determined by the prior knowledge about the parameter. Second, the optimal value is bounded due to the presence of the energy constraint.

IV. Special Case: Optimal Sensor Collaboration for The Estimation of Uncorrelated Parameters

In this section, we show that (P1) can be transformed into a special nonconvex optimization problem, where the difference of convex (DC) functions carries all the nonconvexity. Spurred by the problem structure, we employ a convex-concave procedure (CCP) to solve (P1).

A. Equivalent optimization problem

We express (P1) in its epigraph form [39, Sections 3.1&7.5]

$$\begin{aligned}&\text{minimize} && \mathbf{1}^T\mathbf{u} && \text{(18a)}\\ &\text{subject to} && \frac{\sigma_\epsilon^2\mathbf{w}_k^T\mathbf{R}_k\mathbf{w}_k + \sigma_\varsigma^2}{\mathbf{w}_k^T\mathbf{S}_k\mathbf{w}_k + \sigma_\varsigma^2} \le u_k,\ k \in [K] && \text{(18b)}\\ &&& \mathbf{w}^T\mathbf{Q}_m\mathbf{w} \le E_m, \qquad m \in [M], && \text{(18c)}\end{aligned}$$

where $\mathbf{u} = [u_1, u_2, \ldots, u_K]^T$ is the vector of newly introduced optimization variables.

We further introduce new variables r_k and s_k for $k \in [K]$ to rewrite (18b) as

$$\begin{cases}\dfrac{r_k}{s_k} \le u_k,\ s_k > 0 \\ \mathbf{w}_k^T\mathbf{S}_k\mathbf{w}_k + \sigma_\varsigma^2 \ge s_k \\ \sigma_\epsilon^2\mathbf{w}_k^T\mathbf{R}_k\mathbf{w}_k + \sigma_\varsigma^2 \le r_k,\end{cases} \tag{19}$$

where the equivalence between (18b) and (19) holds since the minimization of $\mathbf{1}^T\mathbf{u}$ with the above inequalities forces the variable s_k and r_k to achieve their upper and lower bounds, respectively.

In (19), the ratio $r_k/s_k \le u_k$ together with $s_k > 0$ can be reformulated as a quadratic inequality of DC type

$$s_k^2 + u_k^2 + 2r_k - (s_k + u_k)^2 \le 0, \tag{20}$$

where both $s_k^2+u_k^2+2r_k$ and $(s_k+u_k)^2$ are convex quadratic functions.

From (19) and (20), problem (18) becomes

$$\begin{aligned}
\text{minimize} \quad & \mathbf{1}^T\mathbf{u} && && \text{(21a)}\\
\text{subject to} \quad & s_k^2+u_k^2+2r_k \le (s_k+u_k)^2, && k\in[K] && \text{(21b)}\\
& s_k-\mathbf{w}_k^T\mathbf{S}_k\mathbf{w}_k-\sigma_\varsigma^2\le 0, && k\in[K] && \text{(21c)}\\
& \sigma_\epsilon^2\mathbf{w}_k^T\mathbf{R}_k\mathbf{w}_k+\sigma_\varsigma^2\le r_k, && k\in[K] && \text{(21d)}\\
& \mathbf{w}^T\mathbf{Q}_m\mathbf{w}\le E_m, && m\in[M] && \text{(21e)}\\
& \mathbf{s}>\mathbf{0}, && && \text{(21f)}
\end{aligned}$$

where the optimization variables are $\mathbf{w}$, $\mathbf{u}$, $\mathbf{r}$ and $\mathbf{s}$, $\mathbf{r}=[r_1,r_2,\ldots,r_K]^T$, $\mathbf{s}=[s_1,s_2,\ldots,s_K]^T$, and $>$ denotes elementwise inequality. Note that the quadratic functions of DC type in (21b) and (21c) contain the nonconvexity of problem (21). In what follows, we will show that CCP is a suitable convex restriction approach for solving this problem.

B. Convex restriction

Problem (21) is convex except for the nonconvex quadratic constraints (21b) and (21c), which have the DC form

$$f(\mathbf{v})-g(\mathbf{v})\le 0, \tag{22}$$

where both f and g are convex functions. In (21b), we have $f(s_k,u_k,r_k)=s_k^2+u_k^2+2r_k$, and $g(s_k,u_k)=(s_k+u_k)^2$. In (21c), $f(s_k)=s_k$, and $g(\mathbf{w}_k)=\mathbf{w}_k^T\mathbf{S}_k\mathbf{w}_k+\sigma_\varsigma^2$.

We can convexify (22) by linearizing g around a feasible point $\hat{\mathbf{v}}$,

$$f(\mathbf{v})-\hat{g}(\mathbf{v})\le 0, \tag{23}$$

where $\hat{g}(\mathbf{v}):=g(\hat{\mathbf{v}})+(\frac{\partial g(\hat{\mathbf{v}})}{\partial \mathbf{v}})^T(\mathbf{v}-\hat{\mathbf{v}})$, $\frac{\partial g(\hat{\mathbf{v}})}{\partial \mathbf{v}}$ is the first-order derivative of g at the point $\hat{\mathbf{v}}$. In (23), $\hat{g}$ is an affine *lower bound* on the convex function g, and therefore, the set of $\mathbf{v}$ that satisfy (23) is a strict *subset* of the set of $\mathbf{v}$ that satisfy (22). This implies that a solution of the optimization problem with the linearized constraint (23) is locally optimal for the problem with the original nonconvex constraint (22).

We can obtain a restricted convex version of problem (21) by linearizing (21b) and (21c) as was done in (22) and (23). We then solve a sequence of convex programs with iteratively updated linearization points. The use of linearization to convexify nonconvex problems with DC type functions is known as CCP [34]. At each iteration of CCP, we solve

$$\begin{aligned}
\text{minimize} \quad & \mathbf{1}^T\mathbf{u}\\
\text{subject to} \quad & s_k^2+u_k^2+2r_k-\hat{g}_1(s_k,u_k)\le 0, && k\in[K]\\
& s_k-\hat{g}_2(\mathbf{w}_k)\le 0, && k\in[K]\\
& \sigma_\epsilon^2\mathbf{w}_k^T\mathbf{R}_k\mathbf{w}_k+\sigma_\varsigma^2\le r_k, && k\in[K]\\
& \mathbf{w}^T\mathbf{Q}_m\mathbf{w}\le E_m, && m\in[M]\\
& \mathbf{s}>\mathbf{0},
\end{aligned} \tag{24}$$

where the optimization variables are $\mathbf{w}$, $\mathbf{u}$, $\mathbf{r}$, and $\mathbf{s}$, $\hat{g}_1$ and $\hat{g}_2$ are affine approximations of $(s_k+u_k)^2$ and $\mathbf{w}_k^T\mathbf{S}_k\mathbf{w}_k+\sigma_\varsigma^2$, namely, $\hat{g}_1(s_k,u_k):=2(\hat{s}_k+\hat{u}_k)(s_k+u_k)-(\hat{s}_k+\hat{u}_k)^2$, and $\hat{g}_2(\mathbf{w}_k):=2\hat{\mathbf{w}}_k^T\mathbf{S}_k\mathbf{w}_k-\hat{\mathbf{w}}_k^T\mathbf{S}_k\hat{\mathbf{w}}_k+\sigma_\varsigma^2$. We summarize CCP for solving problem (21) or (P1) in Algorithm 1.

Algorithm 1 CCP for solving (P1)

Require: initial points $\hat{\mathbf{w}}$, $\hat{\mathbf{s}}$ and $\hat{\mathbf{u}}$, and $\epsilon_{\text{ccp}}>0$

1: **for** iteration $t=1,2,\ldots$ **do**
2: solve problem (24) for the solution $(\mathbf{w}^t,\mathbf{s}^t,\mathbf{u}^t)$
3: update the linearization point, $\hat{\mathbf{w}}=\mathbf{w}^t$, $\hat{\mathbf{s}}=\mathbf{s}^t$, and $\hat{\mathbf{u}}=\mathbf{u}^t$
4: **until** $|\mathbf{1}^T\mathbf{u}^t-\mathbf{1}^T\mathbf{u}^{t-1}|\le\epsilon_{\text{ccp}}$ with $t\ge 2$.
5: **end for**

To initialize Algorithm 1, we can choose random points, for example drawn from a standard uniform distribution, that are then scaled to satisfy the constraints (21b)–(21e). Our extensive numerical examples show that Algorithm 1 is fairly robust with respect to the choice of the initial point; see Fig. 4-(a) for an example.

It is known from [40, Theorem 10] that CCP is a descent algorithm that converges to a stationary point of the original nonconvex problem. To be specific, at each iteration, we solve a restricted convex problem with a smaller feasible set which contains the linearization point (i.e., the solution after the previous iteration). Therefore, we always obtain a new feasible point with a lower or equal objective value. Moreover, reference [41] showed that CCP has *at least* linear convergence rate $O(1/t)$, where t is the number of iterations[1]. However, our numerical results and those in [33], [34], [42] have shown that the empirical convergence rate is typically faster, and much of the benefit of using CCP is gained during its first few iterations.

The computation cost of Algorithm 1 is dominated by the solution of the convex program with quadratic constraints at Step 2. This has the computational complexity $O(a^3+a^2b)$ in the use of interior-point algorithm [43, Chapter 10], where a and b denote the number of optimization variables and constraints, respectively. In problem (24), we have $a=3K+KL$ and $b=4K+M$. Therefore, the complexity of our algorithm is roughly given by $O(L^3)$ per iteration. Here we focus on the scenario in which the number of collaboration links L is much larger than K or M.

V. General Case: Optimal Sensor Collaboration for The Estimation of Correlated Parameters

Different from (P1), the presence of temporal correlation makes finding the solution of (P2) more challenging. However, we demonstrate that (P2) can be recast as an optimization problem with the important property that the problem becomes a semidefinite program (SDP) if its rank-one constraint is replaced by a linear relaxation/approximation. Spurred by the problem structure, we employ a *penalty CCP* to solve (P2), and propose a fast optimization algorithm by using the alternating direction method of multipliers (ADMM).

[1]Given the stopping tolerance ϵ_{ccp}, the linear convergence rate implies $O(1/\epsilon_{\text{ccp}})$ iterations to convergence.

A. Equivalent optimization problem

We transform (P2) into the following equivalent form

$$\begin{aligned} \text{minimize} \quad & \mathrm{tr}(\mathbf{V}) \\ \text{subject to} \quad & \mathbf{P}_w^{-1} \succeq \mathbf{V}^{-1} \\ & \mathbf{w}^T \mathbf{Q}_m \mathbf{w} \leq E_m, \quad m \in [M], \end{aligned} \tag{25}$$

where $\mathbf{V} \in \mathbb{S}^K$ is the newly introduced optimization variable, $\mathbb{S}^n$ represents the set of $n \times n$ symmetric matrices, and the notation $\mathbf{X} \succeq \mathbf{Y}$ (or $\mathbf{X} \preceq \mathbf{Y}$) indicates that $\mathbf{X} - \mathbf{Y}$ (or $\mathbf{Y} - \mathbf{X}$) is positive semidefinite. The first inequality constraint of problem (25) is obtained from $\mathbf{P}_w \preceq \mathbf{V}$, where $\mathbf{P}_w$ is given by (17), and $\mathbf{P}_w^{-1}$ represents the Bayesian Fisher information matrix.

We further introduce a new vector of optimization variables $\mathbf{p} = [p_1, \ldots, p_K]^T$ such that the first matrix inequality of problem (25) is expressed as

$$\mathbf{C} - \mathrm{diag}(\mathbf{p}) \succeq \mathbf{V}^{-1}, \tag{26}$$

$$p_k \geq \sigma_\epsilon^{-2} \mathbf{h}_k^T \left(\mathbf{I} + \sigma_\epsilon^2 \sigma_\varsigma^{-2} \mathbf{G}_k^T \mathbf{U}_k \mathbf{G}_k \right)^{-1} \mathbf{h}_k, \ k \in [K], \tag{27}$$

$$\mathbf{U}_k = \mathbf{w}_k \mathbf{w}_k^T, \tag{28}$$

where we use the expression of $\mathbf{P}_w$ given by (17), and $\mathbf{U}_k \in \mathbb{S}^L$ is the newly introduced optimization variable for $k \in [K]$. Note that the minimization of $\mathrm{tr}(\mathbf{V})$ with inequalities (26) and (27) would force the variable p_k to achieve its lower bound. In other words, problem (25) is equivalent to the problem in which the first inequality constraint of (25) is replaced by the above two inequalities.

By employing the Schur complement, we can express (26) and (27) as the linear matrix inequalities (LMIs)

$$\begin{bmatrix} \mathbf{C} - \mathrm{diag}(\mathbf{p}) & \mathbf{I} \\ \mathbf{I} & \mathbf{V} \end{bmatrix} \succeq 0, \tag{29}$$

$$\begin{bmatrix} p_k & \sigma_\epsilon^{-1} \mathbf{h}_k^T \\ \sigma_\epsilon^{-1} \mathbf{h}_k & \mathbf{I} + \sigma_\epsilon^2 \sigma_\varsigma^{-2} \mathbf{G}_k^T \mathbf{U}_k \mathbf{G}_k \end{bmatrix} \succeq 0, \ k \in [K]. \tag{30}$$

Replacing the first inequality of problem (25) with LMIs (29)–(30), we obtain an optimization problem that is convex except for the rank-one constraint (28), which can be recast as two inequalities

$$\mathbf{U}_k - \mathbf{w}_k \mathbf{w}_k^T \succeq 0, \ \mathbf{U}_k - \mathbf{w}_k \mathbf{w}_k^T \preceq 0, \ k \in [K]. \tag{31}$$

According to the Shur complement, the first matrix inequality is equivalent to the LMI

$$\begin{bmatrix} \mathbf{U}_k & \mathbf{w}_k \\ \mathbf{w}_k^T & 1 \end{bmatrix} \succeq 0, \ k \in [K]. \tag{32}$$

And the second inequality in (31) involves a function of DC type, where $\mathbf{U}_k$ and $\mathbf{w}_k \mathbf{w}_k^T$ are matrix convex functions [39].

From (29)–(32), problem (25) or (P2) is equivalent to

$$\begin{aligned} \text{minimize} \quad & \mathrm{tr}(\mathbf{V}) && \text{(33a)} \\ \text{subject to} \quad & \mathbf{w}^T \mathbf{Q}_m \mathbf{w} \leq E_m, \quad m \in [M] && \text{(33b)} \\ & \text{LMIs in (29)–(30)} && \text{(33c)} \\ & \text{LMIs in (32)} && \text{(33d)} \\ & \mathbf{U}_k - \mathbf{w}_k \mathbf{w}_k^T \preceq 0, \quad k \in [K], && \text{(33e)} \end{aligned}$$

where the optimization variables are $\mathbf{w}$, $\mathbf{p}$, $\mathbf{V}$ and $\mathbf{U}_k$ for $k \in [K]$, and (33e) is a nonconvex constraint of DC type.

B. Convexification

Proceeding with the same logic as in Sec. IV to convexify the constraint (22), we linearize (33e) around a point $\hat{\mathbf{w}}_k$,

$$\mathbf{U}_k - \hat{\mathbf{w}}_k \mathbf{w}_k^T - \mathbf{w}_k \hat{\mathbf{w}}_k^T + \hat{\mathbf{w}}_k \hat{\mathbf{w}}_k^T \preceq 0, \ k \in [K]. \tag{34}$$

It is straightforward to apply CCP to solve problem (33) by replacing (33e) with (34). However, such an approach fails in practice. This is not surprising, since the feasible set determined by (33d) and (34) only contains the linearization point. Specifically, from (33d) and (34), we obtain

$$\begin{aligned} & (\mathbf{w}_k - \hat{\mathbf{w}}_k)(\mathbf{w}_k - \hat{\mathbf{w}}_k)^T \\ &= \mathbf{w}_k \mathbf{w}_k^T - \hat{\mathbf{w}}_k \mathbf{w}_k^T - \mathbf{w}_k \hat{\mathbf{w}}_k^T + \hat{\mathbf{w}}_k \hat{\mathbf{w}}_k^T \\ &\preceq \mathbf{U}_k - \hat{\mathbf{w}}_k \mathbf{w}_k^T - \mathbf{w}_k \hat{\mathbf{w}}_k^T + \hat{\mathbf{w}}_k \hat{\mathbf{w}}_k^T \ \preceq \ 0, \end{aligned} \tag{35}$$

which indicates that $\mathbf{w}_k = \hat{\mathbf{w}}_k$. Therefore, CCP gets trapped in the linearization point.

Remark 3: Dropping the nonconvex constraint (33e) is another method to convexify problem (33), known as semidefinite relaxation [44]. However, such an approach makes the optimization variable $\mathbf{U}_k$ unbounded, since the minimization of $\mathrm{tr}(\mathbf{V})$ forces $\mathbf{U}_k$ to be as large as possible such that the variable p_k in (27) is as small as possible.

In order to circumvent the drawback of the standard CCP, we consider its penalized version, known as penalty CCP [34], [45], where we add new variables to allow for constraints (34) to be violated and penalize the sum of the violations in the objective function. As a result, the convexification (34) is modified by

$$\mathbf{U}_k - \hat{\mathbf{w}}_k \mathbf{w}_k^T - \mathbf{w}_k \hat{\mathbf{w}}_k^T + \hat{\mathbf{w}}_k \hat{\mathbf{w}}_k^T \preceq \mathbf{Z}_k, \ k \in [K], \tag{36}$$

where $\mathbf{Z}_k \in \mathbb{S}^L$ is a newly introduced variable. The constraint (36) implicitly adds the additional constraint $\mathbf{Z}_k \succeq 0$ due to $\mathbf{U}_k \succeq \mathbf{w}_k \mathbf{w}_k$ from (33d).

After replacing (33e) with (36), we obtain the SDP,

$$\begin{aligned} \text{minimize} \quad & \mathrm{tr}(\mathbf{V}) + \tau \sum_{k=1}^{K} \mathrm{tr}(\mathbf{Z}_k) \\ \text{subject to} \quad & \text{(33b)–(33d) and (36)} \end{aligned} \tag{37}$$

where the optimization variables are $\mathbf{w}$, $\mathbf{p}$, $\mathbf{V}$, $\mathbf{U}_k$ and $\mathbf{Z}_k$ for $k \in [K]$, and $\tau > 0$ is a penalty parameter. Compared to the standard CCP, problem (37) is optimized over a larger feasible set since we allow for constraints to be violated by adding variables $\mathbf{Z}_k$ for $k \in [K]$. We summarize the use of penalty CCP to solve (P2) in Algorithm 2.

In Algorithm 2, the initial point $\hat{\mathbf{w}}$ is randomly picked from a standard uniform distribution. Note that $\hat{\mathbf{w}}$ is not necessarily feasible for (P2) since violations of constraints are allowed. We also remark that once $\tau = \tau_{\max}$ (after at most $\log_\mu(\tau_{\max}/\tau_0)$ iterations), the penalty CCP reduces to CCP. Therefore, the penalty CCP enjoys the same convergence properties of CCP.

The computation cost of Algorithm 2 is dominated by the solution of the SDP (37) at Step 2. This leads to the complexity $O(a^2b^2 + ab^3)$ by using the interior-point alogrithm in off-the-shelf solvers [43, Chapter 11], where a and b are the number of optimization variables and the size of the semidefinite matrix, respectively. In (37), the number of optimization variables is

Algorithm 2 Penalty CCP for solving (P2)

Require: an initial point $\hat{\mathbf{w}}$, $\epsilon_{\rm ccp} > 0$, $\tau^0 > 0$, $\tau_{\max} > 0$ and $\mu > 1$.

1: **for** iteration $t = 1, 2, \ldots$ **do**
2: solve problem (37) for its solution $\mathbf{w}^t$ via SDP solver or ADMM-based algorithm in Sec. V-C
3: update the linearization point, $\hat{\mathbf{w}} = \mathbf{w}^t$
4: update the penalty parameter $\tau^t = \min\{\mu\tau^{t-1}, \tau_{\max}\}$
5: let ψ^t be the objective value of (37)
6: **until** $|\psi^t - \psi^{t-1}| \leq \epsilon_{\rm ccp}$ with $t \geq 2$.
7: **end for**

proportional to L^2. Therefore, the complexity of Algorithm 2 is roughly given by $O(L^6)$. Clearly, computing solutions to SDPs becomes inefficient for problems of medium or large size. In what follows, we will develop an ADMM-based algorithm that is more amenable to large-scale optimization.

C. Fast algorithm via ADMM

It has been shown in [35], [46]–[48] that ADMM is a powerful tool for solving large-scale optimization problems. The major advantage of ADMM is that it allows us to split the original problem into subproblems, each of which can be solved more efficiently or even analytically. In what follows, we will employ ADMM to solve problem (37).

It is shown in Appendix B that problem (37) can be reformulated in a way that lends itself to the application of ADMM. This is achieved by introducing slack variables and indicator functions to express the inequality constraints of problem (37) as linear equality constraints together with cone constraints with respect to slack variables, including second-order cone and positive semidefinite cone constraints.

ADMM is performed based on the augmented Lagrangian [35] of the reformualted problem (37), and leads to two problems, the first of which can be treated as an unconstrained quadratic program and the latter renders an analytical solution. These two problems are solved iteratively and communicate to each other through special quadratic terms in their objectives; the quadratic term in each problem contains information about the solution of the other problem and also about dual variables (also known as Lagrange multipliers). In what follows, we refer to these problems as the '$\mathscr{X}$-minimization' and '$\mathscr{Z}$-minimization' problems. Here $\mathscr{X}$ denotes the set of primal variables $\mathbf{w}$, $\mathbf{p}$, $\mathbf{V}$, $\mathbf{U}_k$ and $\mathbf{Z}_k$ for $k \in [K]$, and $\mathscr{Z}$ denotes the set of slack variables $\boldsymbol{\lambda}_m$, $\boldsymbol{\Lambda}_1$ and $\{\boldsymbol{\Lambda}_{i,k}\}_{i=2,3,4}$ for $m \in [M]$ and $k \in [K]$. We also use $\mathscr{Y}$ to denote the set of dual variables $\boldsymbol{\pi}_m$, $\boldsymbol{\Pi}_1$ and $\{\boldsymbol{\Pi}_{i,k}\}_{i=2,3,4}$ for $m \in [M]$ and $k \in [K]$. The ADMM algorithm is precisely described by (58) – (60) in Appendix B.

We emphasize that the crucial property of the ADMM approach is that, as we demonstrate in the rest of this section, the solution of each of the $\mathscr{X}$- and $\mathscr{Z}$-minimization problems can be found exactly and efficiently.

1) $\mathscr{X}$-minimization step: The $\mathscr{X}$-minimization problem can be cast as

$$\text{minimize} \quad \varphi(\mathbf{w}, \mathbf{p}, \mathbf{V}, \{\mathbf{U}_k\}, \{\mathbf{Z}_k\}). \tag{38}$$

The objective function of problem (38) is given by (39), where $\boldsymbol{\alpha}_m := \boldsymbol{\lambda}_m^t - \mathbf{c}_m - (1/\rho)\boldsymbol{\pi}_m^t$ for $m \in [M]$, $\boldsymbol{\Upsilon}_1 := \boldsymbol{\Lambda}_1^t - (1/\rho)\boldsymbol{\Pi}_1^t$, and $\boldsymbol{\Upsilon}_{i,k} := \boldsymbol{\Lambda}_{i,k}^t - (1/\rho)\boldsymbol{\Pi}_{i,k}^t$ for $i \in \{2,3,4\}$ and $k \in [K]$, and t denotes the ADMM iteration. For ease of notation, we will omit the ADMM iteration index t in what follows.

We note that problem (38) is an unconstrained quadratic program (UQP) with large amounts of variables. In order to reduce the computational complexity and memory requirement in optimization, we will employ a gradient descent method [39] together with a backtracking line search [39, Chapter 9.2] to solve this UQP. In Proposition 1, we show the gradient of the objective function of problem (38).

Proposition 1: The gradient of the objective function of problem (38) is given by

$$\begin{aligned}
\nabla_{\mathbf{w}}\varphi &= \rho\textstyle\sum_{m=1}^{M} \bar{\mathbf{Q}}_m^T(\bar{\mathbf{Q}}_m\mathbf{w} - \boldsymbol{\alpha}_m) + 2\rho(\mathbf{w} - \boldsymbol{\gamma}_3) \\
&\quad + 2\rho\,\mathrm{blkdiag}\{\hat{\mathbf{w}}_k\mathbf{w}_k^T + \mathbf{w}_k\hat{\mathbf{w}}_k^T - \mathbf{H}_k\}_{k=1}^K\hat{\mathbf{w}} \\
\nabla_{\mathbf{p}}\varphi &= 2\rho\mathbf{p} + \rho(\mathrm{diag}(\boldsymbol{\Upsilon}_1^{11}) - \mathrm{diag}(\mathbf{C}) - \boldsymbol{\gamma}_2) \\
\nabla_{\mathbf{V}}\varphi &= \mathbf{I} + \rho(\mathbf{V} - \boldsymbol{\Upsilon}_1^{22}) \\
\nabla_{\mathbf{U}_k}\varphi &= \rho\sigma_\epsilon^2\sigma_\varsigma^{-2}\mathbf{G}_k(\mathbf{I} + \sigma_\epsilon^2\sigma_\varsigma^{-2}\mathbf{G}_k^T\mathbf{U}_k\mathbf{G}_k - \boldsymbol{\Upsilon}_{2,k}^{22})\mathbf{G}_k^T \\
&\quad + \rho(2\mathbf{U}_k - \boldsymbol{\Upsilon}_{3,k}^{11} - \mathbf{Z}_k - \mathbf{T}_k),\ k \in [K] \\
\nabla_{\mathbf{Z}_k}\varphi &= \tau\mathbf{I} + \rho(\mathbf{Z}_k - \mathbf{U}_k + \mathbf{T}_k),\ k \in [K],
\end{aligned}$$

where $\boldsymbol{\gamma}_3 = [\boldsymbol{\gamma}_{3,1}^T, \ldots, \boldsymbol{\gamma}_{3,K}^T]^T$, $\boldsymbol{\gamma}_{3,k}$ is the $(L+1)$ column of $\boldsymbol{\Upsilon}_{3,k}$ after the last entry is removed, $\mathbf{H}_k := \mathbf{U}_k - \mathbf{Z}_k + \hat{\mathbf{w}}_k\hat{\mathbf{w}}_k^T + \boldsymbol{\Upsilon}_{4,k}$, $\hat{\mathbf{w}} = [\hat{\mathbf{w}}_1^T, \ldots, \hat{\mathbf{w}}_K^T]^T$, $\boldsymbol{\Upsilon}_1^{11}$ is a submatrix of $\boldsymbol{\Upsilon}_1$ that contains its first K rows and columns, $\boldsymbol{\gamma}_2 = [\gamma_{2,1}, \ldots, \gamma_{2,K}]^T$, $\gamma_{2,k}$ is the first element of $\boldsymbol{\Upsilon}_{2,k}$, $\mathrm{diag}(\cdot)$ returns the diagonal entries of its matrix argument in vector form, $\boldsymbol{\Upsilon}_1^{22}$ is a submatrix of $\boldsymbol{\Upsilon}_1$ after the first K rows and columns are removed, $\boldsymbol{\Upsilon}_{2,k}^{22}$ is a submatrix of $\boldsymbol{\Upsilon}_{2,k}$ after the first row and column are removed, $\boldsymbol{\Upsilon}_{3,k}^{11}$ is a submatrix of $\boldsymbol{\Upsilon}_{3,k}$ after the last row and column are removed, and $\mathbf{T}_k := \hat{\mathbf{w}}_k\mathbf{w}_k^T + \mathbf{w}_k\hat{\mathbf{w}}_k^T - \hat{\mathbf{w}}_k\hat{\mathbf{w}}_k^T - \boldsymbol{\Upsilon}_{4,k}$.

Proof: See Appendix C. ■

In Proposition 1, the optimal values of $\mathbf{p}$ and $\mathbf{V}$ are achieved by letting $\nabla_{\mathbf{p}}\varphi = \mathbf{0}$ and $\nabla_{\mathbf{V}}\varphi = \mathbf{0}$, which yield

$$\mathbf{p} = \frac{1}{2}(\mathrm{diag}(\mathbf{C}) + \boldsymbol{\gamma}_2 - \mathrm{diag}(\boldsymbol{\Upsilon}_1^{11})),\ \mathbf{V} = \boldsymbol{\Upsilon}_1^{22} - \frac{1}{\rho}\mathbf{I}. \tag{40}$$

To solve problem (38) for other variables, we employ the gradient descent method summarized in Algorithm 3. This algorithm calls on the backtracking line search (Algorithm 4) to properly determine the step size such that the convergence to a stationary point of problem (38) is accelerated.

2) $\mathscr{Z}$-minimization step: The $\mathscr{Z}$-minimization problem is decomposed with respect to each of slack variables.

- Subproblem with respect to $\boldsymbol{\lambda}_m$:

$$\begin{array}{ll} \text{minimize} & \|\boldsymbol{\lambda}_m - \boldsymbol{\beta}_m\|_2^2 \\ \text{subject to} & \|[\boldsymbol{\lambda}_m]_{1:KL}\|_2 \leq [\boldsymbol{\lambda}_m]_{KL+1}, \end{array} \tag{41}$$

where $\boldsymbol{\beta}_m := \bar{\mathbf{Q}}_m\mathbf{w}^{t+1} + \mathbf{c}_m + (1/\rho)\boldsymbol{\pi}_m^t$, and t is the ADMM iteration index. For notational simplicity, the ADMM iteration will be omitted in what follows. The solution of problem (41) is achieved by projecting $\boldsymbol{\beta}_m$ onto a second-order cone [46,

$$\varphi(\mathbf{w},\mathbf{p},\mathbf{V},\{\mathbf{U}_k\},\{\mathbf{Z}_k\}) := \mathrm{tr}(\mathbf{V}) + \tau\sum_{k=1}^{K}\mathrm{tr}(\mathbf{Z}_k) + \frac{\rho}{2}\sum_{m=1}^{M}\left\|\bar{\mathbf{Q}}_m\mathbf{w}-\boldsymbol{\alpha}_m\right\|_2^2 + \frac{\rho}{2}\left\|\begin{bmatrix}\mathbf{C}-\mathrm{diag}(\mathbf{p}) & \mathbf{I}\\ \mathbf{I} & \mathbf{V}\end{bmatrix} - \boldsymbol{\Upsilon}_1\right\|_F^2$$
$$+\frac{\rho}{2}\sum_{k=1}^{K}\left\|\begin{bmatrix}p_k & \sigma_\epsilon^{-1}\mathbf{h}_k^T\\ \sigma_\epsilon^{-1}\mathbf{h}_k & \mathbf{I}+\sigma_\epsilon^2\sigma_\varsigma^{-2}\mathbf{G}_k^T\mathbf{U}_k\mathbf{G}_k\end{bmatrix} - \boldsymbol{\Upsilon}_{2,k}\right\|_F^2 + \frac{\rho}{2}\sum_{k=1}^{K}\left\|\begin{bmatrix}\mathbf{U}_k & \mathbf{w}_k\\ \mathbf{w}_k^T & 1\end{bmatrix} - \boldsymbol{\Upsilon}_{3,k}\right\|_F^2$$
$$+\frac{\rho}{2}\sum_{k=1}^{K}\left\|\mathbf{Z}_k-\mathbf{U}_k+\hat{\mathbf{w}}_k\mathbf{w}_k^T+\mathbf{w}_k\hat{\mathbf{w}}_k^T-\hat{\mathbf{w}}_k\hat{\mathbf{w}}_k^T-\boldsymbol{\Upsilon}_{4,k}\right\|_F^2 \tag{39}$$

Algorithm 3 Gradient descent method for solving UQP (38)

Require: values of $\mathbf{w}$, $\{\mathbf{U}_k\}$ and $\{\mathbf{Z}_k\}$ at the previous ADMM iteration, $\mathbf{p}$ and $\mathbf{V}$ given by (40), and $\epsilon_{\mathrm{grad}} > 0$

repeat
  compute the gradient of ϕ following Proposition 1
  compute $c_{\mathrm{grad}} := \sum_{k=1}^{K}\|\nabla_{\mathbf{U}_k}\varphi\|_F^2 + \|\nabla_{\mathbf{w}}\varphi\|_2^2 + \sum_{k=1}^{K}\|\nabla_{\mathbf{Z}_k}\varphi\|_F^2$
  call Algorithm 4 to determine a step size κ
  update variables $\mathbf{w} := \mathbf{w} + \kappa\nabla_{\mathbf{w}}\varphi$, $\mathbf{U}_k := \mathbf{U}_k + \kappa\nabla_{\mathbf{U}_k}\varphi$, $\mathbf{Z}_k := \mathbf{Z}_k + \kappa\nabla_{\mathbf{Z}_k}\varphi$
until $c_{\mathrm{grad}} \le \epsilon_{\mathrm{grad}}$.

Algorithm 4 Backtracking line search for choosing κ

Given $\kappa := 1$, $a_1 \in (0, 0.5)$, $a_2 \in (0,1)$, and c_{grad}
repeat
  $\kappa := a_2\kappa$,
  let $\hat{\varphi}$ be the value of φ at the points $\mathbf{w} + \kappa\nabla_{\mathbf{w}}\varphi$, $\mathbf{U}_k + \kappa\nabla_{\mathbf{U}_k}\varphi$, and $\mathbf{Z}_k + \kappa\nabla_{\mathbf{Z}_k}\varphi$
until $\hat{\varphi} < \varphi(\mathbf{w},\{\mathbf{U}_k\},\{\mathbf{Z}_k\}) - a_1\kappa\, c_{\mathrm{grad}}$.

Sec. 6.3],

$$\boldsymbol{\lambda}_m = \begin{cases}\mathbf{0} & \|[\boldsymbol{\beta}_m]_{1:KL}\|_2 \le -[\boldsymbol{\beta}_m]_{KL+1}\\ \boldsymbol{\beta}_m & \|[\boldsymbol{\beta}_m]_{1:KL}\|_2 \le [\boldsymbol{\beta}_m]_{KL+1}\\ \tilde{\boldsymbol{\beta}}_m & \|[\boldsymbol{\beta}_m]_{1:KL}\|_2 \ge |[\boldsymbol{\beta}_m]_{KL+1}|,\end{cases} \tag{42}$$

for $m \in [M]$, where

$$\tilde{\boldsymbol{\beta}}_m = \frac{1}{2}\left(1+\frac{[\boldsymbol{\beta}_m]_{KL+1}}{\|[\boldsymbol{\beta}_m]_{1:KL}\|_2}\right)\left[[\boldsymbol{\beta}_m]_{1:KL}^T, \|[\boldsymbol{\beta}_m]_{1:KL}\|_2\right]^T.$$

- Subproblem with respect to $\boldsymbol{\Lambda}_1$:

$$\begin{array}{ll}\text{minimize} & \|\boldsymbol{\Lambda}_1 - \boldsymbol{\Phi}_1\|_F^2\\ \text{subject to} & \boldsymbol{\Lambda}_1 \succeq 0,\end{array} \tag{43}$$

where $\boldsymbol{\Phi}_1 := \begin{bmatrix}\mathbf{C}-\mathrm{diag}(\mathbf{p}) & \mathbf{I}\\ \mathbf{I} & \mathbf{V}\end{bmatrix} + (1/\rho)\boldsymbol{\Pi}_1$. The solution of problem (43) is given by [46, Sec. 6.3]

$$\boldsymbol{\Lambda}_1 = \sum_{i=1}^{2K}(\sigma_i)_+\boldsymbol{\omega}_i\boldsymbol{\omega}_i^T, \tag{44}$$

where $\sum_{i=1}^{2K}\sigma_i\boldsymbol{\omega}_i\boldsymbol{\omega}_i^T$ is the eigenvalue decomposition of $\boldsymbol{\Phi}_1$, and $(\cdot)_+$ is the positive part operator.

- Subproblem with respect to $\boldsymbol{\Lambda}_{i,k}$ for $i \in \{2,3,4\}$ and $k \in [K]$:

$$\begin{array}{ll}\text{minimize} & \|\boldsymbol{\Lambda}_{i,k} - \boldsymbol{\Phi}_{i,k}\|_F^2\\ \text{subject to} & \boldsymbol{\Lambda}_{i,k} \succeq 0,\end{array} \tag{45}$$

where

$$\boldsymbol{\Phi}_{2,k} := \begin{bmatrix}p_k & \sigma_\epsilon^{-1}\mathbf{h}_k^T\\ \sigma_\epsilon^{-1}\mathbf{h}_k & \mathbf{I}+\sigma_\epsilon^2\sigma_\varsigma^{-2}\mathbf{G}_k^T\mathbf{U}_k\mathbf{G}_k\end{bmatrix} + \tfrac{1}{\rho}\boldsymbol{\Pi}_{2,k}$$
$$\boldsymbol{\Phi}_{3,k} := \begin{bmatrix}\mathbf{U}_k & \mathbf{w}_k\\ \mathbf{w}_k^T & 1\end{bmatrix} + \tfrac{1}{\rho}\boldsymbol{\Pi}_{3,k}$$
$$\boldsymbol{\Phi}_{4,k} := \mathbf{Z}_k - \mathbf{U}_k + \hat{\mathbf{w}}_k\mathbf{w}_k^T + \mathbf{w}_k\hat{\mathbf{w}}_k^T - \hat{\mathbf{w}}_k\hat{\mathbf{w}}_k^T + \tfrac{1}{\rho}\boldsymbol{\Pi}_{4,k}.$$

The solution of problem (45) is the same as (44) except that $\boldsymbol{\Phi}_1$ is replaced with $\boldsymbol{\Phi}_{i,k}$ for $i \in \{2,3,4\}$ and $k \in [K]$.

3) Summary of the proposed ADMM algorithm: We initialize the ADMM algorithm by setting $\mathbf{w}^0 = \mathbf{1}$, $\mathbf{p}^0 = \mathbf{1}$, $\mathbf{V}^0 = \mathbf{I}$, $\mathbf{U}_k^0 = \mathbf{Z}_k^0 = \mathbf{I}$ for $k \in [K]$, $\boldsymbol{\lambda}_m^0 = \boldsymbol{\pi}_m^0 = \mathbf{0}$ for $m \in [M]$, $\boldsymbol{\Lambda}_1^0 = \boldsymbol{\Pi}_1^0 = \mathbf{0}$, and $\boldsymbol{\Lambda}_{i,k}^0 = \boldsymbol{\Pi}_{i,k}^0 = \mathbf{0}$ for $i \in \{2,3,4,\}$ and $k \in [K]$. The ADMM approach is summarized in Algorithm 5.

Algorithm 5 ADMM for solving problem (37)

Initialize variables and set ρ and ϵ_{admm}
for iteration $t = 1, 2, \ldots$ **do**
  obtain optimal values of primal variables $\mathscr{X}^t$ using Algorithm 3 and (40)
  obtain optimal values of slack variables $\mathscr{Z}^t$ using (42), (44) and (45)
  update dual variables based on (60)
  until both $\|\mathscr{X}^{t+1} - \mathscr{Z}^t\|_F$ and $\|\mathscr{Z}^{t+1} - \mathscr{Z}^t\|_F$ are less than ϵ_{admm}.
end for

The global convergence of ADMM has been widely studied in [49]–[51]. It is known from [49]–[51] that ADMM has a linear convergence rate $O(1/t)$ for general convex optimization problems such as problem (37), where t is the number of iterations. In practice, our numerical results and those in [35], [46]–[48] have shown that ADMM can converge to modest accuracy–sufficient for many applications–within a few tens of iterations.

At each iteration of ADMM, the computational complexity of the $\mathscr{X}$-minimization step is approximated by $O(L^4)$, where $O(L)$ roughly counts for the number of iterations of the gradient descent method, and $O(L^3)$ is the complexity of matrix multiplication while computing the gradient. Here we assume that L is much larger than K and N. In $\mathscr{Z}$-minimization step, the computational complexity is dominated by the eigenvalue decomposition used in (44). This leads to the complexity $O(L^{3.5})$. As a result, the total computation cost of the ADMM algorithm is given by $O(L^4)$. For additional perspective, we compare the computational complexity of

the ADMM algorithm with the interior-point algorithm that takes complexity $O(L^6)$. The complexity of ADMM decreases significantly in terms of the number of collaboration links by a factor L^2. We refer the reader to Sec. VI for numerical results on the running time improvement.

VI. Numerical Results

This section empirically shows the effectiveness of our approach for sensor collaboration in time-varying sensor networks. We assume that θ_k follows a Ornstein-Uhlenbeck process [20] with correlation $\mathrm{cov}(\theta_{k_1}, \theta_{k_2}) = \sigma_\theta^2 e^{-|k_1-k_2|/\rho_{\mathrm{corr}}}$ for $k_1 \in [K]$ and $k_2 \in [K]$, where ρ_{corr} is a parameter that governs the correlation strength, namely, a larger (or smaller) ρ_{corr} corresponds to a weaker (or stronger) correlation. The covariance matrix of $\boldsymbol{\theta}$ is given by

$$\boldsymbol{\Sigma}_{\boldsymbol{\theta}} = \sigma_\theta^2 \begin{bmatrix} 1 & e^{-\rho_{\mathrm{corr}}} & \cdots & e^{-(K-1)\rho_{\mathrm{corr}}} \\ e^{-\rho_{\mathrm{corr}}} & 1 & \cdots & e^{-(K-2)\rho_{\mathrm{corr}}} \\ \vdots & \vdots & \ddots & \vdots \\ e^{-(K-1)\rho_{\mathrm{corr}}} & e^{-(K-2)\rho_{\mathrm{corr}}} & \cdots & 1 \end{bmatrix}.$$

where unless specified otherwise, we set $\sigma_\theta^2 = 1$ and $\rho_{\mathrm{corr}} = 0.5$. The spatial placement and neighborhood structure of the sensor network is modeled by a random geometric graph [18], $\mathrm{RGG}(N, d)$, where $N = 10$ sensors are randomly deployed over a unit square and *bidirectional* communication links are possible only for pairwise distances at most d. Clearly, the topology matrix $\mathbf{A}$ is determined by $\mathrm{RGG}(N, d)$, and the number of collaboration links increases as d increases. In our numerical examples unless specified otherwise, we set $d = 0.3$ which leads to $\mathrm{RGG}(10, 0.3)$ shown in Fig. 3.

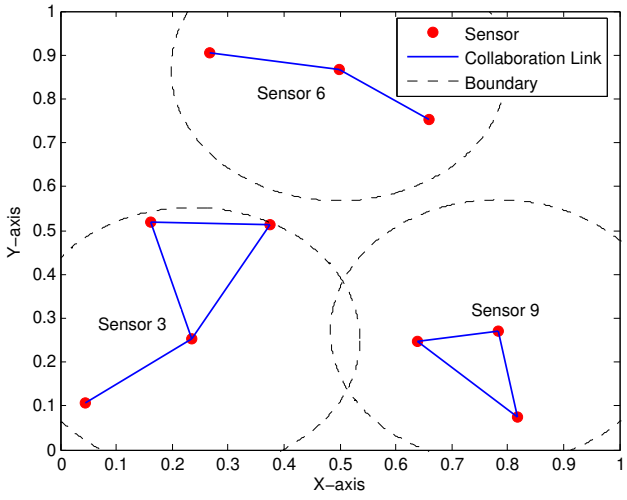

Fig. 3: $\mathrm{RGG}(10, 0.3)$, collaboration is depicted for sensors 3, 6 and 9.

In the collaborative estimation system shown in Fig. 1, we assume that $M = N$, $K = 3$, $\sigma_\epsilon^2 = \sigma_\varsigma^2 = 1$, and $E_m = E_{\mathrm{total}}/M$ for $m \in [M]$, where $E_{\mathrm{total}} = 1$ gives the total energy budget of M sensors. For simplicity, the obverstion gain $\mathbf{h}_k$ and channel gain $\mathbf{g}_k$ are randomly chosen from the uniform distribution $\mathcal{U}(0.1, 1)$. Moreover, we select $\tau^0 = 0.1$, $\mu = 1.5$, $\tau_{\max} = 100$ in penalty CCP (namely, Algorithm 2), $a_1 = 0.02$ and $a_2 = 0.5$ in backtracking line search (namely, Algorithm 4) and $\epsilon_{\mathrm{ccp}} = \epsilon_{\mathrm{admm}} = \epsilon_{\mathrm{grad}} = 10^{-3}$ for the stopping tolerance of the proposed algorithms. Unless specified otherwise, the ADMM algorithm is adopted at Step 2 of penalty CCP, and we use CVX [52] for all other computations. The estimation performance is measured through the empirical mean squared error (MSE), which is computed over 1000 numerical trials.

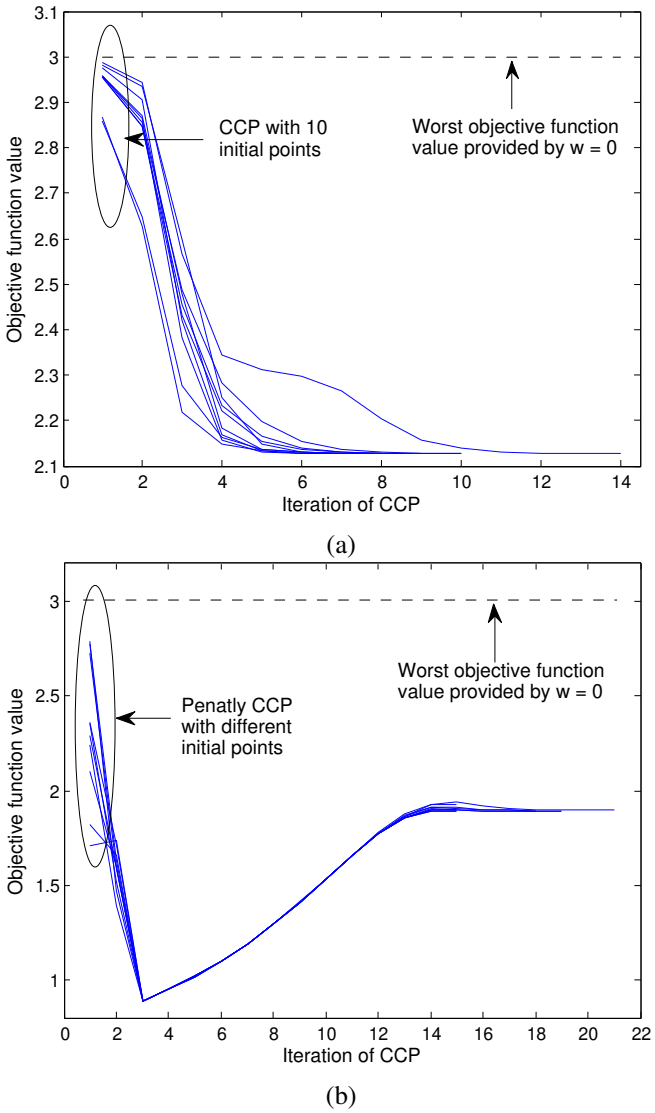

Fig. 4: Convergence of Algorithm 1 and 2 for different initial points.

In Fig. 4, we present convergence trajectories of CCP (namely, Algorithm 1) and penalty CCP (namely, Algorithm 2) as functions of interation index for 10 different initial points. For comparison, we plot the worst objective function value of collaboration problem (7) when $\mathbf{w} = \mathbf{0}$, namely, LMMSE is determined only by the prior information, which leads to the worst estimation error $\mathrm{tr}(\boldsymbol{\Sigma}_\theta) = K = 3$. As we can see, much of the benefit of using CCP or penalty CCP is gained during the first few iterations. And each algorithm converges to almost the same objective function value for different initial points. Compared to CCP, the convergence trajectory of penalty CCP is not monotonically decreasing. Namely, penalty CCP is not

a descent algorithm. The non-monotonicity of penalty CCP is caused by the penalization on the violation of constraints in the objective function. The objective function value of penalty CCP converges until the penalization ceases to change significantly (after 15 iterations in this example).

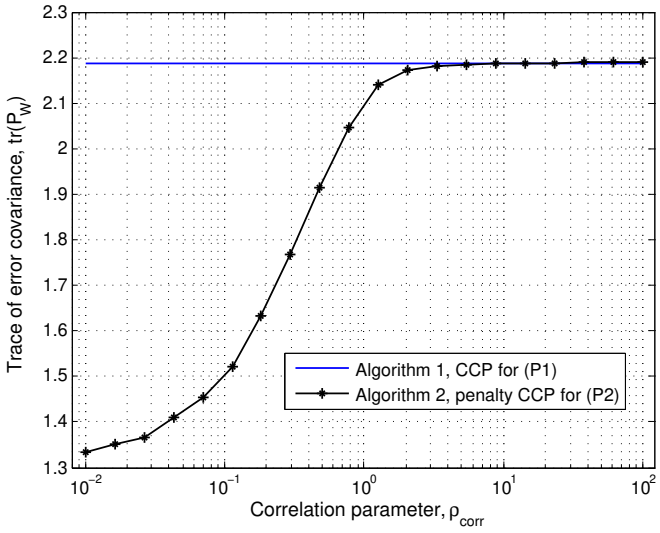

Fig. 5: Estimation error versus correlation parameter ρ_{corr}.

In Fig. 5, we present the trace of error covariance matrix $\mathbf{P}_W$ given by (5) as a function of the correlation parameter ρ_{corr}, where the sensor collaboration scheme is obtained from Algorithm 1 and Algorithm 2 to solve (P1) and (P2), respectively. We observe that the estimation error resulting from the solution of (P1) remains unchanged for different values of ρ_{corr} since the formulation of (P1) is independent of the prior knowledge about parameter correlation. The estimation error resulting from the solution of (P2) increases as ρ_{corr} increases, and it eventually converges to the error resulting from the solution of (P1) at an extremely large ρ_{corr}, where parameters become uncorrelated. This is not surprising, since the prior information about parameter correlation was taken into account in (P2), thereby significantly improving the estimation performance.

In Fig. 6, we present the MSE of collaborative estimation as a function of the total energy budget E_{total} for $\rho_{\text{corr}} = 0.5$. For comparison, we plot the estimation performance when using a time-invariant collaboration scheme to solve (P1) and (P2), respectively. The assumption of time-invariant collaboration implicitly adds the additional constraint $\mathbf{w}_1 = \ldots = \mathbf{w}_K$, which reduces the problem size. By fixing the type of algorithm, we observe that the MSE when using time-invariant sensor collaboration is larger than that of the originally proposed algorithm. This is because the latter accounts for temporal dynamics of the network, where observation and channel gains vary in time. Moreover, the solution of (P2) yields lower MSE than that of (P1). This result is consistent with Fig. 5 for a fixed correlation parameter. Lastly, the estimation error is smaller as more energy is used in sensor collaboration.

In Fig. 7, we present the MSE and the number of collaboration links as functions of the collaboration radius d for $\rho_{\text{corr}} = 0.5$ and $E_{\text{total}} = 1$. We note that the estimation

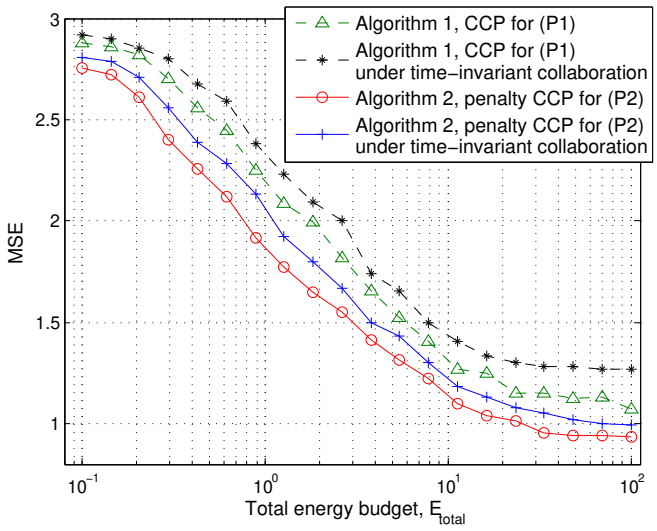

Fig. 6: MSE versus total energy budget.

accuracy improves as d increases, since a larger value of d corresponds to more collaboration links in the network. For a fixed value of d, the MSE when solving (P2) is lower than that when solving (P1), since the latter ignores the information about parameter correlation. Moreover, we observe that the MSE tends to saturate beyond a collaboration radius $d \approx 0.7$. This indicates that a large part of the performance improvement is achieved only through partial collaboration.

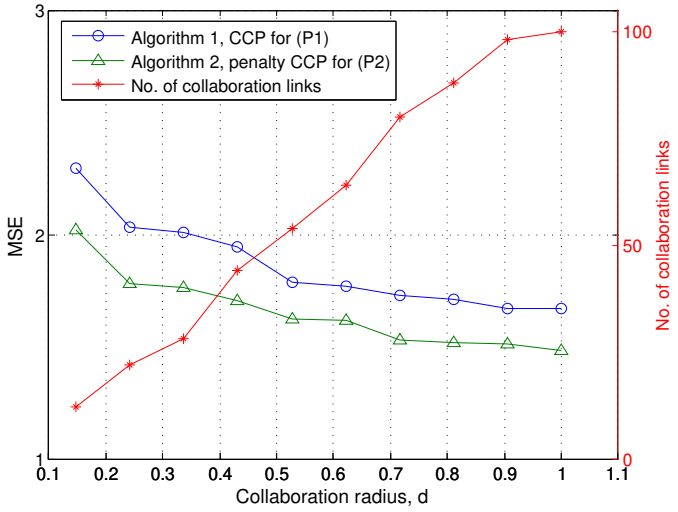

Fig. 7: MSE and collaboration links versus collaboration radius d.

In Fig. 8, we present the MSE as a function of the signal-to-noise ratio (SNR), $10\log_{10}(\sigma_\theta^2/\sigma_v^2)$, where $\sigma_\theta^2 = 1$ is the variance of the parameter to be estimated, and $\sigma_v^2 \in [10^{-3}, 10^3]$ is the variance of the additive communication noise when inter-sensor collaboration occurs. In this numerical example, we study the impact of *noisy* collaboration links on estimation performance, where the collaboration scheme is obtained by the solution of (P2) for $d \in \{0.5, 1\}$. As we can see, estimation distortion increases when SNR decreases. Moreover, the MSE in the presence of noisy collaboration under the lowest SNR is consistent with that of using the classical amplify-and-forward

transmission strategy in the absence of sensor collaboration. This is because each sensor has access to its own measurement in a noiseless manner (collaboration noise only occurs if two different sensors are communicating). At a fixed value of SNR, we observe that the MSE decreases as d increases, and it converges to the MSE in the absence of collaboration noise. This implies that the act of sensor collaboration is able to improve estimation performance even if the collaboration link is noisy.

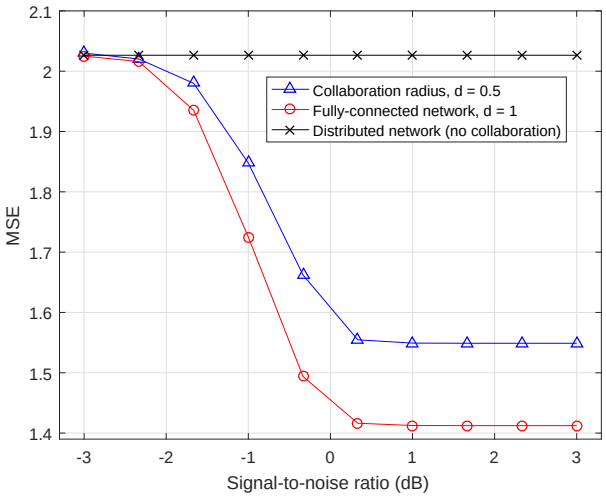

Fig. 8: Noisy collaboration: MSE versus SNR.

In Fig. 9, we present the computation time of our algorithms as functions of problem size specified in terms of the number of collaboration links L. For comparison, we plot the computation time of penalty CCP when using an interior-point solver in CVX [52]. As we can see, penalty CCP requires much higher computation time than CCP, since the former requires solutions of SDPs. When L is small, we observe that the ADMM based penalty CCP has a higher computation time than when using the interior-point solver. This is because the gradient descent method in ADMM takes relatively more iterations (compared to small L) to converge with satisfactory accuracy. However, the ADMM based algorithm performs much faster for a relatively large problem with $L > 80$.

VII. Conclusions

We study the problem of sensor collaboration for estimation of time-varying parameters in sensor networks. Based on prior knowledge about parameter correlations, the resulting sensor collaboration problem is solved for estimation of temporally uncorrelated and correlated parameters. In the case of temporally uncorrelated parameters, we show that the sensor collaboration problem can be cast as a special nonconvex optimization problem, where a difference of convex functions carries all the nonconvexity. By exploiting problem structure, we solve the problem by using a convex-concave procedure, which renders a good locally optimal solution as evidenced by numerical results. In the case of correlated parameters, we show that the sensor collaboration problem can be converted into a semidefinite program together with a

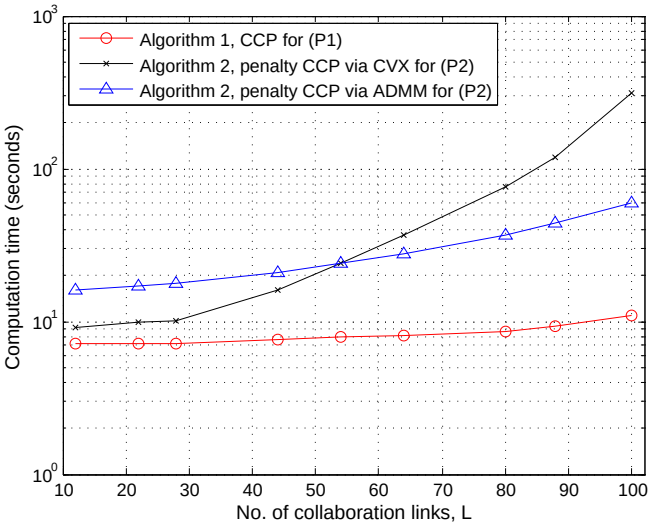

Fig. 9: Computation time versus number of collaboration links.

nonconvex rank-one constraint. Spurred by problem structure, we employ a semidefinite programming based penalty convex-concave procedure to solve the sensor collaboration problem. Moreover, we propose an ADMM-based algorithm that scales more gracefully for large problems. Numerical results are provided to demonstrate the effectiveness of our approach and the impact of parameter correlation and temporal dynamics of sensor networks on the performance of distributed estimation with sensor collaboration.

There are multiple directions for future research. We would like to consider noise-corrupted or quantization-based imperfect communication links in sensor collaboration. It will also be of interest to seek the duality gap between the nonconvex sensor collaboration problems in order to gain theoretical insights on the performance of the proposed optimization methods. Another direction of future work is to seek an approach that jointly designs the optimal power allocation scheme and the collaboration topology. Last but not the least, it will be worthwhile to study the sensor collaboration problem in the framework of consensus-based decentralized estimation.

Appendix A
Proof of Equation (10)

Let $\mathbf{w} \in \mathbb{R}^L$ be the vector of stacking the *nonzero* entries of $\mathbf{W} \in \mathbb{R}^{M\times N}$ columnwise. We note that there exists a one-to-one mapping between the element of $\mathbf{w}$ and the nonzero entry of $\mathbf{W}$. That is, given w_l for $l \in [L]$, we have a certain pair of indices (m_l, n_l) such that $w_l = W_{m_l n_l}$, where $m_l \in [M]$ and $n_l \in [N]$. Moreover, we obtain that

$$W_{ij} = 0, \text{ if } (i,j) \notin \mathcal{I} , \tag{46}$$

where $\mathcal{I} := \{(m_l, n_l)\}_{l=1}^L$.

Given $\mathbf{b} \in \mathbb{R}^M$, we have

$$\mathbf{b}^T\mathbf{W} = \left[\sum_{i=1}^M b_i W_{i1} \quad \cdots \quad \sum_{i=1}^M b_i W_{iN}\right].$$

Given $\mathbf{B} \in \mathbb{R}^{L\times N}$, we obtain

$$\mathbf{w}^T\mathbf{B} = \begin{bmatrix} \sum_{l=1}^{L} B_{l1}W_{m_l n_l} & \cdots & \sum_{l=1}^{L} B_{lN}W_{m_l n_l} \end{bmatrix},$$

where we used the fact that $w_l = W_{m_l n_l}$.

Consider the tth entry of $\mathbf{w}^T\mathbf{B}$ for $t \in [N]$, we obtain

$$\begin{aligned}[\mathbf{w}^T\mathbf{B}]_t &= \sum_{l=1}^{L} B_{lt}W_{m_l n_l} = \sum_{l=1, n_l=t}^{L} b_{m_l}W_{m_l t} \\ &= \sum_{m_l=1}^{M} b_{m_l}W_{m_l t} = [\mathbf{b}^T\mathbf{W}]_t, \end{aligned} \tag{47}$$

where we used the facts that $B_{lt} = \begin{cases} b_{m_l} & t = n_l \\ 0 & \text{otherwise} \end{cases}$ for $(m_l, n_l) \in \mathcal{I}$, and $W_{m_l t} = 0$ if $(m_l, t) \notin \mathcal{I}$. Based on (47), we can conclude that $\mathbf{w}^T\mathbf{B} = \mathbf{b}^T\mathbf{W}$. ■

Appendix B
Application of ADMM

We introduce slack variables $\boldsymbol{\lambda}_m \in \mathbb{R}^{KL+1}$ for $m \in [M]$ to rewrite (33b) as an equality constraint together with a second-order cone constraint,

$$\bar{\mathbf{Q}}_m\mathbf{w} - \boldsymbol{\lambda}_m + \mathbf{c}_m = \mathbf{0}, \ \|[\boldsymbol{\lambda}_m]_{1:KL}\|_2 \le [\boldsymbol{\lambda}_m]_{KL+1}, \tag{48}$$

where $\bar{\mathbf{Q}}_m := [\mathbf{Q}_m^{\frac{1}{2}}, \mathbf{0}]^T$, $\mathbf{Q}_m^{\frac{1}{2}}$ is the square root of $\mathbf{Q}_m$ given by the matrix decomposition $\mathbf{Q}_m = (\mathbf{Q}_m^{\frac{1}{2}})^T\mathbf{Q}_m^{\frac{1}{2}}$, $\mathbf{c}_m = [\mathbf{0}^T, \sqrt{E_m}]^T$, and $[\mathbf{a}]_{1:n}$ denotes a subvector of $\mathbf{a}$ that consists of its first n entries.

We further introduce slack variables $\boldsymbol{\Lambda}_1 \in \mathbb{S}^{2K}$, $\boldsymbol{\Lambda}_{2,k} \in \mathbb{S}^{N+1}$, $\boldsymbol{\Lambda}_{3,k} \in \mathbb{S}^{L+1}$ and $\boldsymbol{\Lambda}_{4,k} \in \mathbb{S}^{L}$ for $k \in [K]$ to rewrite LMIs of problem (37) as a sequence of equality constraints together with positive semidefinite cone constraints

$$\begin{bmatrix} \mathbf{C} - \operatorname{diag}(\mathbf{p}) & \mathbf{I} \\ \mathbf{I} & \mathbf{V} \end{bmatrix} - \boldsymbol{\Lambda}_1 = \mathbf{0} \tag{49}$$

$$\begin{bmatrix} p_k & \sigma_\epsilon^{-1}\mathbf{h}_k^T \\ \sigma_\epsilon^{-1}\mathbf{h}_k & \mathbf{I} + \sigma_\epsilon^2\sigma_\varsigma^{-2}\mathbf{G}_k^T\mathbf{U}_k\mathbf{G}_k \end{bmatrix} - \boldsymbol{\Lambda}_{2,k} = \mathbf{0} \tag{50}$$

$$\begin{bmatrix} \mathbf{U}_k & \mathbf{w}_k \\ \mathbf{w}_k^T & 1 \end{bmatrix} - \boldsymbol{\Lambda}_{3,k} = \mathbf{0} \tag{51}$$

$$\mathbf{Z}_k - \mathbf{U}_k + \hat{\mathbf{w}}_k\mathbf{w}_k^T + \mathbf{w}_k\hat{\mathbf{w}}_k^T - \hat{\mathbf{w}}_k\hat{\mathbf{w}}_k^T - \boldsymbol{\Lambda}_{4,k} = \mathbf{0}, \tag{52}$$

where $\boldsymbol{\Lambda}_1 \succeq 0$, $\boldsymbol{\Lambda}_{2,k} \succeq 0$, $\boldsymbol{\Lambda}_{3,k} \succeq 0$, and $\boldsymbol{\Lambda}_{4,k} \succeq 0$ for $k \in [K]$.

From (48)–(52), problem (37) becomes

$$\begin{aligned} \text{minimize} \quad & \operatorname{tr}(\mathbf{V}) + \tau\sum_{k=1}^{K}\operatorname{tr}(\mathbf{Z}_k) + \sum_{m=1}^{M}\mathcal{I}_0(\boldsymbol{\lambda}_m) \\ & + \mathcal{I}_1(\boldsymbol{\Lambda}_1) + \sum_{i=2}^{4}\sum_{k=1}^{K}\mathcal{I}_i(\boldsymbol{\Lambda}_{i,k}) \\ \text{subject to} \quad & \text{equality constraints in (48)–(52)}, \end{aligned} \tag{53}$$

where the optimization variables are $\mathbf{w}$, $\mathbf{p}$, $\mathbf{V}$, $\mathbf{U}_k$, $\mathbf{Z}_k$, $\boldsymbol{\lambda}_m$, $\boldsymbol{\Lambda}_1$, and $\{\boldsymbol{\Lambda}_{i,k}\}_{i=2,3,4}$ for $m \in [M]$ and $k \in [K]$, and $\mathcal{I}_i$ is the indicator function specified by

$$\mathcal{I}_0(\boldsymbol{\lambda}_m) = \begin{cases} 0, & \text{if } \|[\boldsymbol{\lambda}_m]_{1:KL}\|_2 \le [\boldsymbol{\lambda}_m]_{KL+1} \\ \infty & \text{otherwise}, \end{cases} \tag{54}$$

$$\mathcal{I}_1(\boldsymbol{\Lambda}_1) = \begin{cases} 0, & \text{if } \boldsymbol{\Lambda}_1 \succeq 0 \\ \infty & \text{otherwise}, \end{cases} \tag{55}$$

$$\mathcal{I}_i(\boldsymbol{\Lambda}_{i,k}) = \begin{cases} 0, & \text{if } \boldsymbol{\Lambda}_{i,k} \succeq 0 \\ \infty & \text{otherwise}, \end{cases} \quad i = 2,3,4. \tag{56}$$

It is clear from problem (53) that the introduced indicator functions helps to isolate the second-order cone and positive semidefinite cone constraints with respect to slack variables.

Problem (53) is now in a form suitable for the application of ADMM. The corresponding augmented Lagrangian [35] in ADMM is given by

$$\begin{aligned} \mathcal{L}_\rho(\mathscr{X}, \mathscr{Z}, \mathscr{Y}) &= \operatorname{tr}(\mathbf{V}) + \tau\sum_{k=1}^{K}\operatorname{tr}(\mathbf{Z}_k) + \sum_{m=1}^{M}\mathcal{I}_0(\boldsymbol{\lambda}_m) \\ &+ \mathcal{I}_1(\boldsymbol{\Lambda}_1) + \sum_{i=2}^{4}\sum_{k=1}^{K}\mathcal{I}_i(\boldsymbol{\Lambda}_{i,k}) + \sum_{m=1}^{M}\boldsymbol{\pi}_m^T\mathbf{f}_m(\mathscr{X}, \mathscr{Z}) \\ &+ \frac{\rho}{2}\sum_{m=1}^{M}\|\mathbf{f}_m(\mathscr{X}, \mathscr{Z})\|_2^2 + \operatorname{tr}\left(\boldsymbol{\Pi}_1^T\mathbf{F}_1(\mathscr{X}, \mathscr{Z})\right) \\ &+ \frac{\rho}{2}\|\mathbf{F}_1(\mathscr{X}, \mathscr{Z})\|_F^2 + \sum_{i=2}^{4}\sum_{k=1}^{K}\operatorname{tr}\left(\boldsymbol{\Pi}_{i,k}^T\mathbf{F}_{i,k}(\mathscr{X}, \mathscr{Z})\right) \\ &+ \frac{\rho}{2}\sum_{i=2}^{4}\sum_{k=1}^{K}\|\mathbf{F}_{i,k}(\mathscr{X}, \mathscr{Z})\|_F^2, \end{aligned} \tag{57}$$

where $\mathscr{X}$ denotes the set of primal variables $\mathbf{w}$, $\mathbf{p}$, $\mathbf{V}$, $\mathbf{U}_k$ and $\mathbf{Z}_k$ for $k \in [K]$, $\mathscr{Z}$ denotes the set of primal slack variables $\boldsymbol{\lambda}_m$, $\boldsymbol{\Lambda}_1$ and $\{\boldsymbol{\Lambda}_{i,k}\}_{i=2,3,4}$ for $m \in [M]$ and $k \in [K]$, $\mathscr{Y}$ is the set of dual variables $\boldsymbol{\pi}_m$, $\boldsymbol{\Pi}_1$ and $\{\boldsymbol{\Pi}_{i,k}\}_{i=2,3,4}$ for $m \in [M]$ and $k \in [K]$, $\mathbf{f}_m(\cdot)$, $\mathbf{F}_1(\cdot)$, and $\mathbf{F}_{i,k}(\cdot)$ for $i \in \{2,3,4\}$ represent linear functions at the left hand side of equality constraints in (48)–(52), $\rho > 0$ is a regularization parameter, and $\|\cdot\|_F$ denotes the Frobenius norm of a matrix.

We iteratively execute the following three steps for ADMM iteration $t = 0, 1, \ldots$

$$\mathscr{X}^{t+1} = \arg\min_{\mathscr{X}} \mathcal{L}(\mathscr{X}, \mathscr{Z}^t, \mathscr{Y}^t) \tag{58}$$

$$\mathscr{Z}^{t+1} = \arg\min_{\mathscr{Z}} \mathcal{L}(\mathscr{X}^{t+1}, \mathscr{Z}, \mathscr{Y}^t) \tag{59}$$

$$\begin{cases} \boldsymbol{\pi}_m^{t+1} = \boldsymbol{\pi}_m^t + \rho\,\mathbf{f}_m(\mathscr{X}^{t+1}, \mathscr{Z}^{t+1}), \ \forall m \\ \boldsymbol{\Pi}_1^{t+1} = \boldsymbol{\Pi}_1^t + \rho\,\mathbf{F}_1(\mathscr{X}^{t+1}, \mathscr{Z}^{t+1}) \\ \boldsymbol{\Pi}_{i,k}^{t+1} = \boldsymbol{\Pi}_{i,k}^t + \rho\,\mathbf{F}_{i,k}(\mathscr{X}^{t+1}, \mathscr{Z}^{t+1}), \ \forall i,k, \end{cases} \tag{60}$$

until both of the conditions $\|\mathscr{X}^{t+1} - \mathscr{Z}^t\|_F \le \epsilon_{\text{admm}}$ and $\|\mathscr{Z}^{t+1} - \mathscr{Z}^t\|_F \le \epsilon_{\text{admm}}$ are satisfied, where with an abuse of notation, $\|\mathscr{X}\|_F$ denotes the sum of Frobenius norms of variables in $\mathscr{X}$, and ϵ_{admm} is a stopping tolerance.

Substituting (57) into (58) and completing the squares with respect to primal variables, the $\mathscr{X}$-minimization problem (58) becomes the unconstrained quadratic program given by (38).

Substituting (57) into (59), the $\mathscr{Z}$-minimization problem (59) is decomposed into a sequence of subproblems with respect to each of slack variables, given by (41), (43) and (45). ■

APPENDIX C
PROOF OF PROPOSITION 1

We begin by collecting terms in φ associated with $\mathbf{w}$,

$$\varphi_{\mathbf{w}} :=\frac{\rho}{2}\sum_{m=1}^{M}\left\|\bar{\mathbf{Q}}_m\mathbf{w}-\boldsymbol{\alpha}_m\right\|_2^2+\rho\sum_{k=1}^{K}\|\mathbf{w}_k-\boldsymbol{\gamma}_{3,k}\|_2^2 + \frac{\rho}{2}\sum_{k=1}^{K}\|\hat{\mathbf{w}}_k\mathbf{w}_k^T+\mathbf{w}_k\hat{\mathbf{w}}_k^T-\mathbf{H}_k\|_F^2, \quad (61)$$

where $\boldsymbol{\gamma}_{3,k}$ is the $(L+1)$ column of $\boldsymbol{\Upsilon}_{3,k}$ after the last entry is removed, and $\mathbf{H}_k := \mathbf{U}_k-\mathbf{Z}_k+\hat{\mathbf{w}}_k\hat{\mathbf{w}}_k^T+\boldsymbol{\Upsilon}_{4,k}$, which is a symmetric matrix.

In (61), we assume an incremental change $\delta\mathbf{w}$ in $\mathbf{w}$. Replacing $\mathbf{w}$ with $\mathbf{w}+\delta\mathbf{w}$ and $\varphi_{\mathbf{w}}$ with $\varphi_{\mathbf{w}}+\delta\varphi_{\mathbf{w}}$ and collecting first order variation terms on both sides of (61), we obtain

$$\delta\varphi_{\mathbf{w}} =\rho\sum_{m=1}^{M}(\bar{\mathbf{Q}}_m\mathbf{w}-\boldsymbol{\alpha}_m)^T\bar{\mathbf{Q}}_m\delta\mathbf{w}+2\rho(\mathbf{w}-\boldsymbol{\gamma}_3)^T\delta\mathbf{w} + 2\rho\hat{\mathbf{w}}^T\mathrm{blkdiag}\{\hat{\mathbf{w}}_k\mathbf{w}_k^T+\mathbf{w}_k\hat{\mathbf{w}}_k^T-\mathbf{H}_k\}\delta\mathbf{w}, \quad (62)$$

where $\boldsymbol{\gamma}_3=[\boldsymbol{\gamma}_{3,1}^T,\ldots,\boldsymbol{\gamma}_{3,K}^T]^T$, and $\hat{\mathbf{w}}=[\hat{\mathbf{w}}_1^T,\ldots,\hat{\mathbf{w}}_K^T]^T$. It is clear from (62) that the gradient of φ with respect to $\mathbf{w}$ is given by

$$\nabla_{\mathbf{w}}\varphi =\rho\sum_{m=1}^{M}\bar{\mathbf{Q}}_m^T(\bar{\mathbf{Q}}_m\mathbf{w}-\boldsymbol{\alpha}_m)+2\rho(\mathbf{w}-\boldsymbol{\gamma}_3) + 2\rho\,\mathrm{blkdiag}\{\hat{\mathbf{w}}_k\mathbf{w}_k^T+\mathbf{w}_k\hat{\mathbf{w}}_k^T-\mathbf{H}_k\}\hat{\mathbf{w}}. \quad (63)$$

Second, we collect the terms associated with $\mathbf{p}$ in φ to construct the function

$$\varphi_{\mathbf{p}} := \frac{\rho}{2}\|\mathbf{C}-\mathrm{diag}(\mathbf{p})-\boldsymbol{\Upsilon}_1^{11}\|_F^2+\frac{\rho}{2}\|\mathbf{p}-\boldsymbol{\gamma}_2\|_2^2, \quad (64)$$

where $\boldsymbol{\Upsilon}_1^{11}$ is a matrix that consists of the first K rows and columns of $\boldsymbol{\Upsilon}_1$, and $\boldsymbol{\gamma}_2$ is a vector whose kth entry is given by the first entry of $\boldsymbol{\Upsilon}_{2,k}$ for $k\in[K]$.

In (64), replacing $\mathbf{p}$ with $\mathbf{p}+\delta\mathbf{p}$ and $\varphi_{\mathbf{p}}$ with $\varphi_{\mathbf{p}}+\delta\varphi_{\mathbf{p}}$ and collecting first order variation terms on both sides, we obtain

$$\delta\varphi_{\mathbf{p}}=\rho[2\mathbf{p}+\mathrm{diag}(\boldsymbol{\Upsilon}_1^{11})-\mathrm{diag}(\mathbf{C})-\boldsymbol{\gamma}_2]^T\delta\mathbf{p}, \quad (65)$$

where $\mathrm{diag}(\cdot)$ returns in vector form the diagonal entries of its matrix argument. Therefore, the gradient of φ with respect to $\mathbf{p}$ is given by

$$\nabla_{\mathbf{p}}\varphi=\rho[2\mathbf{p}+\mathrm{diag}(\boldsymbol{\Upsilon}_1^{11})-\mathrm{diag}(\mathbf{C})-\boldsymbol{\gamma}_2]. \quad (66)$$

Third, given the terms associated with $\mathbf{V}$ in φ, the gradient of φ with respect to $\mathbf{V}$ is readily cast as

$$\nabla_{\mathbf{V}}\varphi=\mathbf{I}+\rho(\mathbf{V}-\boldsymbol{\Upsilon}_1^{22}), \quad (67)$$

where $\boldsymbol{\Upsilon}_1^{22}$ is a submatrix of $\boldsymbol{\Upsilon}_1$ after the first K rows and columns are removed.

Further, we collect the terms in φ with respect to the variable $\mathbf{U}_k$, and consider the function

$$\varphi_{\mathbf{U}_k} := \frac{\rho}{2}\left\|\mathbf{I}+\sigma_\epsilon^2\sigma_\varsigma^{-2}\mathbf{G}_k^T\mathbf{U}_k\mathbf{G}_k-\boldsymbol{\Upsilon}_{2,k}^{22}\right\|_F^2 + \frac{\rho}{2}\|\mathbf{U}_k-\boldsymbol{\Upsilon}_{3,k}^{11}\|_F^2+\frac{\rho}{2}\|\mathbf{U}_k-\mathbf{Z}_k-\mathbf{T}_k\|_F^2, \quad (68)$$

where $\boldsymbol{\Upsilon}_{2,k}^{22}$ is a submatrix of $\boldsymbol{\Upsilon}_{2,k}$ after the first row and column are removed, $\boldsymbol{\Upsilon}_{3,k}^{11}$ is a submatrix of $\boldsymbol{\Upsilon}_{3,k}$ after the last row and column are removed, and $\mathbf{T}_k := \hat{\mathbf{w}}_k\mathbf{w}_k^T+\mathbf{w}_k\hat{\mathbf{w}}_k^T-\hat{\mathbf{w}}_k\hat{\mathbf{w}}_k^T-\boldsymbol{\Upsilon}_{4,k}$.

In (68), replacing $\mathbf{U}_k$ with $\mathbf{U}_k+\delta\mathbf{U}_k$ and $\varphi_{\mathbf{U}_k}$ with $\varphi_{\mathbf{U}_k}+\delta\varphi_{\mathbf{U}_k}$ and collecting first order variation terms on both sides, we obtain

$$\delta\varphi_{\mathbf{U}_k}=\frac{\rho\sigma_\epsilon^2}{\sigma_\varsigma^2}\,\mathrm{tr}\left(\mathbf{G}_k(\mathbf{I}+\frac{\sigma_\epsilon^2}{\sigma_\varsigma^2}\mathbf{G}_k^T\mathbf{U}_k\mathbf{G}_k-\boldsymbol{\Upsilon}_{2,k}^{22})^T\mathbf{G}_k^T\delta\mathbf{U}_k\right) + \rho\,\mathrm{tr}\left(\left(\mathbf{U}_k-\boldsymbol{\Upsilon}_{3,k}^{11}\right)^T\delta\mathbf{U}_k+\left(\mathbf{U}_k-\mathbf{Z}_k-\mathbf{T}_k\right)^T\delta\mathbf{U}_k\right).$$

Therefore, the gradient of φ with respect to $\mathbf{U}_k$ is given by

$$\nabla_{\mathbf{U}_k}\varphi =\rho\sigma_\epsilon^2\sigma_\varsigma^{-2}\mathbf{G}_k(\mathbf{I}+\sigma_\epsilon^2\sigma_\varsigma^{-2}\mathbf{G}_k^T\mathbf{U}_k\mathbf{G}_k-\boldsymbol{\Upsilon}_{2,k}^{22})\mathbf{G}_k^T + \rho(\mathbf{U}_k-\boldsymbol{\Upsilon}_{3,k}^{11})+\rho(\mathbf{U}_k-\mathbf{Z}_k-\mathbf{T}_k). \quad (69)$$

Finally, the gradient of φ with respect to $\mathbf{Z}_k$ is given by

$$\nabla_{\mathbf{Z}_k}\varphi=\tau\mathbf{I}+\rho(\mathbf{Z}_k-\mathbf{U}_k+\mathbf{T}_k), \quad (70)$$

where $\mathbf{T}_k$ is defined in (68). We now complete the proof by combining (63), (66), (67), (69) and (70). ■

REFERENCES

[1] L. Oliveira and J. Rodrigues, "Wireless sensor networks: a survey on environmental monitoring," *Journal of Communications*, vol. 6, no. 2, 2011.

[2] Y. Zou and K. Chakrabarty, "Sensor deployment and target localization in distributed sensor networks," *ACM Transactions on Embedded Computing Systems*, vol. 3, no. 1, pp. 61–91, Feb. 2004.

[3] T. He, P. Vicaire, T. Yan, L. Luo, L. Gu, G. Zhou, S. Stoleru, Q. Cao, J. A. Stankovic, and T. Abdelzaher, "Achieving real-time target tracking using wireless sensor networks," in *Proceedings of IEEE Real Time Technology and Applications Symposium*, 2006, pp. 37–48.

[4] S. Cui, J.-J. Xiao, A. J. Goldsmith, Z.-Q. Luo, and H. V. Poor, "Estimation diversity and energy efficiency in distributed sensing," *IEEE Transactions on Signal Processing*, vol. 55, no. 9, pp. 4683–4695, 2007.

[5] J.-J. Xiao, S. Cui, Z.-Q. Luo, and A. J. Goldsmith, "Linear coherent decentralized estimation," *IEEE Transactions on Signal Processing*, vol. 56, no. 2, pp. 757–770, 2008.

[6] S. Marano, V. Matta, L. Tong, and P. Willett, "A likelihood-based multiple access for estimation in sensor networks," *IEEE Transactions on Signal Processing*, vol. 55, no. 11, pp. 5155–5166, Nov. 2007.

[7] A. Sarwate and M. Gastpar, "A little feedback can simplify sensor network cooperation," *IEEE Journal on Selected Areas in Communications*, vol. 28, no. 7, pp. 1159–1168, Sept. 2010.

[8] K. Liu and A. M. Sayeed, "Type-based decentralized detection in wireless sensor networks," *IEEE Transactions on Signal Processing*, vol. 55, no. 5, pp. 1899–1910, May 2007.

[9] G. Mergen, V. Naware, and L. Tong, "Asymptotic detection performance of type-based multiple access over multiaccess fading channels," *IEEE Transactions on Signal Processing*, vol. 55, no. 3, pp. 1081–1092, March 2007.

[10] M. K. Banavar, A. D. Smith, C. Tepedelenlioglu, and A. Spanias, "Distributed detection over fading macs with multiple antennas at the fusion center," in *Proc. IEEE International Conference on Acoustics, Speech and Signal Processing (ICASSP)*, March 2010, pp. 2894–2897.

[11] K. Cohen and A. Leshem, "Performance analysis of likelihood-based multiple access for detection over fading channels," *IEEE Transactions on Information Theory*, vol. 59, no. 4, pp. 2471–2481, April 2013.

[12] J. A. Maya, L. R. Vega, and C. G. Galarza, "Optimal resource allocation for detection of a gaussian process using a mac in wsns," *IEEE Transactions on Signal Processing*, vol. 63, no. 8, pp. 2057–2069, April 2015.

[13] S. Dasarathan and C. Tepedelenlioglu, "Distributed estimation and detection with bounded transmissions over gaussian multiple access channels," *IEEE Transactions on Signal Processing*, vol. 62, no. 13, pp. 3454–3463, July 2014.

[14] J. Fang and H. Li, "Power constrained distributed estimation with cluster-based sensor collaboration," *IEEE Transactions on Wireless Communications*, vol. 8, no. 7, pp. 3822–3832, 2009.

[15] G. Thatte and U. Mitra, "Power allocation in linear and tree wsn topologies," in *Proceedings of Asilomar Conference on Signals, Systems and Computers*, Oct 2006, pp. 1342–1346.

[16] G. Thatte and U. Mitra, "Sensor selection and power allocation for distributed estimation in sensor networks: Beyond the star topology," *IEEE Transactions on Signal Processing*, vol. 56, no. 7, pp. 2649–2661, July 2008.

[17] M. Fanaei, M. C. Valenti, A. Jamalipour, and N. A. Schmid, "Optimal power allocation for distributed blue estimation with linear spatial collaboration," in *Proceedings of IEEE International Conference on Acoustics, Speech and Signal Processing (ICASSP)*, May 2014, pp. 5452–5456.

[18] S. Kar and P. K. Varshney, "Linear coherent estimation with spatial collaboration," *IEEE Transactions on Information Theory*, vol. 59, no. 6, pp. 3532–3553, June 2013.

[19] S. Kar and P. K. Varshney, "On linear coherent estimation with spatial collaboration," in *Proceedings of the 2012 IEEE International Symposium on Information Theory Proceedings (ISIT)*, 2012, pp. 1448–1452.

[20] S. Kar and P. K. Varshney, "Controlled collaboration for linear coherent estimation in wireless sensor networks," in *Proceedings of the 50th Annual Allerton Conference on Communication, Control, and Computing (Allerton)*, 2012, pp. 334–341.

[21] S. Liu, S. Kar, M. Fardad, and P. K. Varshney, "On optimal sensor collaboration topologies for linear coherent estimation," in *Proceedings of IEEE International Symposium on Information Theory (ISIT)*, 2014, pp. 2624–2628.

[22] S. Liu, S. Kar, M. Fardad, and P. K. Varshney, "Sparsity-aware sensor collaboration for linear coherent estimation," *IEEE Transactions on Signal Processing*, vol. 63, no. 10, pp. 2582–2596, May 2015.

[23] M. C. Vuran, O. B. Akan, and I. F. Akyildiz, "Spatio-temporal correlation: theory and applications for wireless sensor networks," *Computer Networks*, vol. 45, no. 3, pp. 245–259, June 2004.

[24] M. C. Vuran and O. B. Akan, "Spatio-temporal characteristics of point and field sources in wireless sensor networks," in *Proc. IEEE International Conference on Communications (ICC)*, June 2006, vol. 1, pp. 234–239.

[25] Phaeton C. Kyriakidis, "A spatial time series framework for modeling daily precipitation at regional scales," *Journal of Hydrology*, vol. 297, no. 4, pp. 236 – 255, Apr. 2004.

[26] S. Kar and J. M. F. Moura, "Distributed consensus algorithms in sensor networks with imperfect communication: Link failures and channel noise," *IEEE Transactions on Signal Processing*, vol. 57, no. 1, pp. 355–369, Jan. 2009.

[27] S. Hosseini, A. Chapman, and M. Mesbahi, "Online distributed estimation via adaptive sensor networks," *http://rain.aa.washington.edu/@api/deki/files/324/=TCNS13_0914_double_column.pdf*, 2014.

[28] S. Shahrampour, A. Rakhlin, and A. Jadbabaie, "Distributed estimation of dynamic parameters : Regret analysis," *https://arxiv.org/abs/1603.00576*, 2016.

[29] R. Olfati-Saber, "Distributed kalman filtering for sensor networks," in *Proc. 46th IEEE Conference on Decision and Control*, Dec. 2007, pp. 5492–5498.

[30] R. Carli, A. Chiuso, L. Schenato, and S. Zampieri, "Distributed kalman filtering based on consensus strategies," *IEEE Journal on Selected Areas in Communications*, vol. 26, no. 4, pp. 622–633, May 2008.

[31] I. D. Schizas, A. Ribeiro, and G. B. Giannakis, "Consensus in ad hoc wsns with noisy links – part i: Distributed estimation of deterministic signals," *IEEE Transactions on Signal Processing*, vol. 56, no. 1, pp. 350–364, Jan. 2008.

[32] I. D. Schizas, G. B. Giannakis, S. I. Roumeliotis, and A. Ribeiro, "Consensus in ad hoc wsns with noisy links – part ii: Distributed estimation and smoothing of random signals," *IEEE Transactions on Signal Processing*, vol. 56, no. 4, pp. 1650–1666, April 2008.

[33] A. L. Yuille and A. Rangarajan, "The concave-convex procedure," *Neural Computation*, vol. 15, no. 4, pp. 915–936, 2003.

[34] T. Lipp and S. Boyd, "Variations and extensions of the convex-concave procedure," http://web.stanford.edu/~boyd/papers/pdf/cvx_ccv.pdf, 2014.

[35] S. Boyd, N. Parikh, E. Chu, B. Peleato, and J. Eckstein, "Distributed optimization and statistical learning via the alternating direction method of multipliers," *Foundations and Trends in Machine Learning*, vol. 3, no. 1, pp. 1–122, 2011.

[36] S. M. Kay, *Fundamentals of Statistical Signal Processing, Volume I: Estimation Theory*, Prentice Hall, Englewood Cliffs, NJ, 1993.

[37] P. Shen, Y. Chen, and Y. Ma, "Solving sum of quadratic ratios fractional programs via monotonic function," *Applied Mathematics and Computation*, vol. 212, no. 1, pp. 234–244, 2009.

[38] F. Bugarin, D. Henrion, and J.-B. Lasserre, "Minimizing the sum of many rational functions," *Mathematical Programming Computation*, pp. 1–29, 2015.

[39] S. Boyd and L. Vandenberghe, *Convex Optimization*, Cambridge University Press, Cambridge, 2004.

[40] B. K. Sriperumbudur and Gert R. G. Lanckriet, "On the convergence of the concave-convex procedure," in *NIPS*, 2009.

[41] Ian E.H. Yen, N. Peng, P.-W. Wang, and S.-D. Lin, "On convergence rate of concave-convex procedure," in *Proc. the NIPS 2012 Optimization Workshop*, 2012.

[42] Q. Kuang, X. Yu, and W. Utschick, "Network topology adaptation and interference coordination for energy saving in heterogeneous networks," in *Proc. IEEE International Conference on Acoustics, Speech and Signal Processing (ICASSP)*, 2016.

[43] A. Nemirovski, "Interior point polynomial time methods in convex programming," 2012 [Online], Available: *http://www2.isye.gatech.edu/~nemirovs/Lect_IPM.pdf*.

[44] Z.-Q. Luo, W.-K. Ma, A. M.-C. So, Y. Ye, and S. Zhang, "Semidefinite relaxation of quadratic optimization problems," *IEEE Signal Processing Magazine*, vol. 27, no. 3, pp. 20–34, May 2010.

[45] M. Fardad and M. R. Jovanović, "On the design of optimal structured and sparse feedback gains via sequential convex programming," in *Proceedings of American Control Conference (ACC)*, June 2014, pp. 2426–2431.

[46] N. Parikh and S. Boyd, "Proximal algorithms," *Foundations and Trends in Optimization*, vol. 1, no. 3, pp. 123–231, 2013.

[47] B. O'Donoghue, E. Chu, N. Parikh, and S. Boyd, "Operator splitting for conic optimization via homogeneous self-dual embedding," Arxiv preprint *http://arxiv.org/abs/1312.3039*, 2013.

[48] Y. Shi, J. Zhang, B. O'Donoghue, and K. B. Letaief, "Large-scale convex optimization for dense wireless cooperative networks," *IEEE Transactions on Signal Processing*, vol. 63, no. 18, pp. 4729–4743, Sept. 2015.

[49] B. He and X. Yuan, "On the $O(1/n)$ convergence rate of the douglasrachford alternating direction method," *SIAM Journal on Numerical Analysis*, vol. 50, no. 2, pp. 700–709, 2012.

[50] W. Deng and W. Yin, "On the global and linear convergence of the generalized alternating direction method of multipliers," *Journal of Scientific Computing*, vol. 66, no. 3, pp. 889–916, 2016.

[51] M. Hong and Z.-Q. Luo, "On the linear convergence of the alternating direction method of multipliers," *http://arxiv.org/abs/1208.3922*, 2013.

[52] Inc. CVX Research, "CVX: Matlab software for disciplined convex programming, version 2.0," *http://cvxr.com/cvx*, Aug 2012.